USGS
science for a changing world

Aeromagnetic Interpretations for Understanding the Hydrogeologic Framework of the Southern Española Basin, New Mexico

By V. J. S. Grauch and Viki Bankey

U.S. Geological Survey, MS 964, Federal Center, Denver, CO 80225-0046

Prepared in cooperation with the

NEW MEXICO OFFICE OF THE STATE ENGINEER

Open-File Report 03-124

2003

U.S. Department of the Interior
U.S. Geological Survey

DISCLAIMERS

Aeromagnetic Interpretations for Understanding the Hydrogeologic Framework of the Southern Española Basin, New Mexico

by

V. J. S. Grauch and Viki Bankey

Open-File Report 03-124

The data contact is: V. J. S. ("Tien") Grauch
303-236-1393
tien@usgs.gov
U. S. Geological Survey, MS 964
Box 25046, Denver Federal Center
Denver, CO 80225 USA

TABLE OF CONTENTS

TABLE OF CONTENTS - CONTINUED

LIST OF TABLES

LIST OF FIGURES

LIST OF PLATES

DIGITAL FILES

Digital files can be accessed from http://pubs.usgs.gov/of/2003/ofr-03-124/

EXECUTIVE SUMMARY

High-resolution aeromagnetic data were flown over the southern Española basin for the purposes of better understanding geologic controls on ground-water flow and storage. This report presents preliminary interpretations of these data. The results depict the presence of and depth to many geologic features that have hydrogeologic significance, including shallow faults, different types of igneous units, and basement rocks. From these results, we can estimate the thickness of Santa Fe Group sediments, which constitute the primary aquifer system for residents of Santa Fe, Española, six Pueblo nations, and surrounding communities.

The interpretations were accomplished using state-of-the-art magnetic-interpretation methods and geophysical profile modeling that incorporated gravity data and other geophysical and geologic constraints. Discussion of the interpretation results is divided by generalized geologic unit: Precambrian basement, Tertiary intrusive rocks and volcanic vents, Oligocene volcanic rocks (layered volcaniclastic and volcanic flow rocks), Pliocene-Quaternary volcanic rocks, Santa Fe Group, and shallow faults. Depths to the Oligocene volcanic rocks are significant because these rocks represent the base of the Santa Fe Group in the southern half of the study area. The following conclusions were reached for the interpreted features.

Precambrian basement

- Depth estimates to the top of the Precambrian basement surface indicate it is more than 10,000' (3048 m) deep in the northwestern part of the study area, declines from 3000' (914 m) depth west and northwest of Santa Fe to >9000' (2743 m) near the eastern side of the Cerros del Rio volcanic field, and is generally 3000-4000' (914-1219 m) deep south of Eldorado.

- The top of the basement surface is variable, but generally dips westward, with dips of 12-15^{o} near the eastern mountain front and 5-20^{o} farther west. In the northeast part of the Eldorado subdivision, basement rises to the surface with an overall dip of 15^{o} to the southwest and plunging more steeply to the southeast.

- Several narrow, north-south elongated aeromagnetic anomalies northwest of Santa Fe can be explained either by structural relief on the basement surface or by fault-controlled Oligocene igneous intrusions that do not require much vertical offset of basement rocks.

- A major difference in basement lithology is indicated north of Santa Fe by a sharp contrast in magnetization along an east-west line, with magnetic basement on the north and weakly magnetic basement on the south.

Tertiary Intrusive Rocks and Volcanic Vents

- The laccolithic Cerrillos intrusion is interpreted to include a wide area surrounding the Cerrillos Hills. The shape of its associated magnetic anomaly indicates the intrusion has fairly steep contacts around all but its western side, suggesting that sills related to the intrusion are generally thin, concentrated at depth only on the western side, or both.

- Many circular, negative magnetic anomalies are associated with volcanic vents related to the Quaternary-Tertiary Cerros del Rio volcanic field. Similar anomalies have sources that are buried and appear related to Oligocene volcanic rocks.

- An area of widespread vents and intrusions is interpreted in the central and western parts of the Cerros del Rio volcanic field.

Oligocene Volcanic Rocks

- Depths to Oligocene volcanic rocks (volcaniclastic rocks and flows) give information on the thickness of the Santa Fe Group because the volcanic rocks directly underlie these sediments over a large part of the study area.

- Depth estimates indicate the Oligocene volcanic rocks are shallow (<250 ft; 75 m) beneath alluvium of the younger Ancha Formation (upper Santa Fe Group) in the southern part of the study area, including the western half of the Eldorado subdivision. This uppermost volcanic surface appears faulted and irregular, with isolated depressions up to 1¼ mile (2 km) wide and 800 ft (245 m) deep that are likely filled with Ancha Formation sediments.

- The volcanic rocks dip northward into the Española basin as an asymmetric, plunging syncline. Depths range from 2000-4000 ft (610-1220 m) west of Santa Fe, and reach more than 7000 ft (2135 m) 5 miles (8 km) south of Buckman Mesa.

- Both explanations for the north-south elongated aeromagnetic anomalies just northwest of Santa Fe (basement-involved structures or fault-controlled igneous intrusion) indicate that Oligocene volcanic rocks shallow abruptly in these areas, causing the Santa Fe Group to thin to perhaps as little as 2000 ft (610 m).

- Variations in aeromagnetic patterns suggest a change in the character of the volcanic rocks roughly northwest and southeast of Gallina Arroyo. On the northwest, the shallowest rocks are dominated by northeast-oriented elongated features, which may be basalt-filled paleochannels, similar to Cieneguilla basaltic rocks exposed near La Cienega. On the southeast, the shallowest volcanic rocks are dominated by volcaniclastic rocks, similar to those of the Espinaso Formation exposed near Galisteo Creek.

- Aeromagnetic patterns also indicate several broad areas where volcanic rocks are absent below the Ancha Formation in the eastern part of Eldorado subdivision, south of the subdivision, and southeast of La Cienega. In these areas, Ancha Formation probably rests directly on older sedimentary rocks, likely the Eocene Galisteo Formation.

Pliocene-Quaternary Volcanic Rocks

- The aeromagnetically determined, lateral extent of the Cerros del Rio volcanic field closely approximates geologically mapped contacts.

- Aeromagnetic analysis shows that the basalts of the Cerros del Rio volcanic field are fairly thin surrounding Buckman Mesa and along the much of the east-central edge of the field.

Santa Fe Group

- The thickness of the Santa Fe Group can be estimated from depths to Oligocene volcanic rocks over most of the central and south-central parts of the study area, as given above.

- Magnetic expression in certain areas indicate that shallow Santa Fe Group sediments are dominated by coarse grain sizes, which can be corroborated by geologic mapping. These areas occur in the northwestern part of the study area corresponding to the Puye Formation, in the central part of the study area, corresponding to the coarse upper units of Tesuque Formation, and generally northeast of the Santa Cruz River.

Shallow Faults

- Aeromagnetic expression of faults that offset Santa Fe Group sediments indicate that major differences in lithology occur on either side of the fault. Thus, recognizing these faults in the aeromagnetic data are important because the contrast in lithology is likely accompanied by a contrast in aquifer properties.

- Faults interpreted from their aeromagnetic expression show generally north to northeast trends where they offset Santa Fe Group sediments in the central and northern parts of the study area. They correspond in general location and trend to mapped faults.

- In the southern part of the area, the aeromagnetic data show linear faults within the expression of the Oligocene volcanic rocks.

Although the aeromagnetic interpretations provide a good preliminary view of many hydrogeologically important features in the southern Española basin, many details are still unresolved. Future work to address these questions might involve drilling, detailed geophysical work using a variety of methods on the ground, revised geologic mapping, rock property measurements, and constructing additional, integrated geophysical models.

INTRODUCTION

Aquifers within the Española basin and adjoining Santa Fe embayment (Fig. 1) are the primary ground-water resource of the City of Santa Fe, Española, six Pueblo nations, and surrounding urbanizing areas. To better define and manage this important ground-water resource, an improved understanding of the subsurface geologic controls on ground-water flow and storage is needed. A valuable tool for improving this understanding is high-resolution aeromagnetic data. Aeromagnetic data are geophysical data acquired from aircraft that measure the subtle variations in the Earth's magnetic field due to differences in the magnetic properties of the underlying rocks. Although aeromagnetic data are insensitive to the presence of water, differing magnetic properties of certain rock types can be detected and used to infer many aspects of the subsurface geology that control the presence, quality, and flow of ground water. Aeromagnetic methods have already proven useful in the Middle Rio Grande basin for efficiently locating subsurface hydrogeologic features, the knowledge of which ultimately improved the ground-water flow model for the basin (Bartolino and Cole, 2002).

High-resolution aeromagnetic data were collected over the southern Española basin in 1998 (Fig. 1; U. S. Geological Survey and others, 1999). Preliminary examination of these data indicated that they could provide significant new information on the depth and lateral extents of Precambrian basement rocks, buried intrusive and volcanic rocks, and shallow faults. These features either directly affect ground water storage, flow, and/or quality, or can be used to infer aquifer thickness, depths to potential aquifers, or problem drilling sites. This report presents interpretations of these features from the high-resolution aeromagnetic data and provides the interpretative line work in digital form. The aeromagnetic results are complemented and improved by other types of information, such as that provided by geologic mapping, hydrologic measurements, exploration wells, and other types of geophysical data. Thus, these results are only the first step towards integration and synthesis with the other data, which will undoubtedly require amendments to the present results.

This report presents brief backgrounds on the aeromagnetic data and the interpretation approaches and methods. The main interpreted features are divided for convenience by geologic age and rock type: Precambrian basement, Tertiary intrusive rocks and volcanic vents, Oligocene volcanic rocks, Pliocene-Quaternary volcanic rocks, and shallow faults. Some discussion of the Santa Fe Group and profile models that incorporate all these features are included in these sections. Within the section on each feature, subsections address the hydrogeologic significance of the feature, its expected magnetic expression, the specific methods of interpretation used, the results of the interpretation, limitations of the results, and recommendations for future work. Finally, the types, formats, and names of the digital interpretative files that accompany this report are described.

HIGH-RESOLUTION AEROMAGNETIC DATA

As part of the Middle Rio Grande Basin study (Bartolino and Cole, 2002), the U. S. Geological Survey acquired high-resolution aeromagnetic surveys that cover most of the Albuquerque basin and southern part of the Española basin, a total area of about 8100 km^2 (Grauch and others, 2001; Sweeney and others, 2002). The data covering the southern Española basin are primarily from the Sandoval-Santa Fe survey, flown with 500 ft (150 m) spacing between east-west lines and at a nominal 500 ft (150 m) height above ground (U. S. Geological Survey and others, 1999). Additional data over the Cochiti Pueblo area (Fig. 1) were flown east-west with ¼-mile (400 m) line spacing and the magnetic sensor at a nominal 240 ft (73 m) above ground (U. S. Geological Survey and others, 1999). After the flight-line data were processed to remove Earth's field variations and reduce common data acquisition errors, the data from the separate surveys were interpolated onto grids with 164 ft (50 m) intervals, analytically continued to a smoothed observation surface 300 ft (100 m) above ground, then digitally merged to gain consistency across the area and enhance details (Sweeney and others, 2002). Finally, the data were reduced to the pole to correct for offsets between the locations of anomalies and their sources (the polarity effect), which is a consequence of the vector nature of the Earth's magnetic field (Blakely, 1995). Assuming that all rocks have magnetizations oriented nearly colinear with the Earth's magnetic field (a good assumption for this study area), reduced-to-pole aeromagnetic data consist of anomalies that are placed directly over their sources.

Plate 1 is a color shaded-relief image of the final, reduced-to-pole aeromagnetic data from Sweeney and others (2002). This image uses color to display the broad variations in the

data and shading (analogous to illumination by the sun) to enhance many subtle details obliquely oriented to the illumination direction.

GENERAL INTERPRETATION METHODS

Aeromagnetic interpretation involves two steps to arrive at a geologic interpretation of the subsurface. The first step is to determine the distribution of magnetization from the magnetic field data, which entails finding the shape and magnetic properties of "sources". The second step is to interpret the magnetic sources in terms of geology. Even though many analytical tools exist to assist in the first step, magnetic data are inherently ambiguous. Thus, the results must be constrained by independent information, simple assumptions, or by reasonable expectations for the area. The second step commonly involves examination of anomaly patterns in relation to topography and exposures of geologic units to determine the aeromagnetic character of a particular geologic unit. This step is fairly subjective and reliant on the quality of the geologic information available and the experience and knowledge of the interpreter. The analytical methods used for magnetic source interpretations are briefly described next. Short explanations of how geologic interpretations were approached for each feature are included in their respective sections below.

Edge Detection

The steepest portions of the sides of gravity or magnetic anomalies are commonly associated with edges of magnetic sources, caused by abrupt lateral rock-property contrasts that occur at faults or steeply dipping contacts. The horizontal-gradient method is commonly used to detect these edges semi-automatically in either gravity or magnetic data. The steepest gradients can be located by finding the local maxima of the magnitudes of the horizontal gradient of gravity data (Cordell, 1979), pseudogravity data (Cordell and Grauch, 1985; Blakely and Simpson, 1986), or reduced-to-pole magnetic data Grauch and others, 2001). The procedure is analogous to taking a derivative to find the inflection point of a curve. Pseudogravity data, or the magnetic potential, is a vertical integral of the reduced-to-pole magnetic data (Baranov, 1957; Blakely, 1995), intuitively similar to taking an average.

Although the horizontal-gradient method using reduced-to-pole aeromagnetic data is extremely useful for detecting magnetic edges, the geologic interpretation of the edges is more difficult. The locations of maxima from the horizontal-gradient method can represent the locations of (1) faults, where a magnetic contrast is produced by structural juxtaposition of units; (2) contacts, where the magnetic contrast is produced by the limit of deposition of a magnetic unit against a less magnetic one; (3) steep topographic slopes, where the magnetic contrast is produced by the interface between rock and air; (4) abrupt changes in magnetization within one rock unit, produced by primary differences in magnetization or due to secondary destruction or growth of magnetic minerals, or (5) an artifact produced by the geometry of a nearby source shaped like a thin sheet. In addition, multiple gradient maxima can occur where thin, horizontal sheet-like sources are vertically offset from thicker sources at depth, called a thin-thick layers model (Grauch and others, 2001). Integration of geologic and topographic information is necessary in order to develop a geologic interpretation of magnetic edges.

Depth Estimation Methods

Methods for estimating depth to magnetic sources from aeromagnetic data rely on the general principle that shallow sources produce anomalies with steep gradients, whereas deep sources produce anomalies with broad gradients. However, source properties also affect anomaly gradients, so that certain shallow sources with wide extent and gradual variations in magnetization can masquerade as deeper sources. Interference of anomalies produced by neighboring or overlying sources also cause difficulties for depth estimation techniques. Depth separation techniques also use anomaly shape to divide the aeromagnetic data into components based on depth. However, sources are commonly present throughout the vertical section, which results in overlap of anomaly content between components.

Methods to estimate depths from magnetic anomalies have been developed in the geophysical literature and can be applied either to profiles extracted from the aeromagnetic data across selected anomalies or to grids by passing a square window across the grid. The computer program PDEPTH (Phillips, 1997) was used to estimate depths along profiles for this study. This program incorporates a variety of methods so that the results of multiple methods can be examined together. This examination is advantageous because no one method works best for all types of sources and at all depths. The primary methods utilized for this study were multi-source Werner (Hansen and Simmonds, 1993), Euler deconvolution (Thompson, 1982), local wave-number or source parameter imaging (Thurston and Smith, 1997; Smith and others, 1998), analytic signal (Nabighian, 1972; 1974), and horizontal-gradient (Roest and Pilkington, 1993; Phillips, 2000). Except for the local wave-number method, which gives a solution for source type directly, the methods give results based on the assumption of a certain source type. Common geologic source types are categorized as thick contacts, such as a fault with great offset or the edge of a pluton, or thin sheets, such as a basalt flow or dike. Although realistically, the shapes can be something in between a thick contact and a thin sheet, such as a fault with moderate offset, or more complicated, such as a fold or a gradational contact, the two simple assumptions of source type can give useful ranges in depths. In practice, the thin sheet assumption is most useful for near-surface sources, because thin sheets at depth require unusually high magnetization in order to produce magnetic anomalies, due to their small volumes. For this study, the assumption of a thick contact source type gave most reasonable results for nearly all situations.

Results from the multiple methods are rarely coincident, for several reasons: (1) anomalies due to neighboring or overlying sources may interfere with each other; (2) geologic sources are much more variable than assumed by any of the methods; (3) these variations produce different types of deviations in results for each method; and (4) the variations, and thus, the likely deviations, are unknown. Thus, determination of final depth estimates from these results was primarily subjective, based on professional knowledge and judgments about the reliability of the methods. A maximum error of ±20% of estimated depth is commonly assumed for magnetic depth estimates (Milsom, 1989).

The horizontal-gradient and local wave-number techniques have been adapted for use across a grid of data (Phillips, 1997). With both techniques, depth estimates are evaluated in a window moving across the grid whenever a linear trend, assumed to represent a contact or fault, is found within the window. Using reduced-to-pole magnetic data as input, the horizontal-

gradient method gives results assuming thick vertical contacts. Using pseudogravity data, the method gives results assuming edges of thin horizontal sheets (Phillips, 2000). Both the horizontal-gradient method (using reduced-to-pole magnetic data) and the local wave-number method give fairly good results for very shallow sources, but the local wave-number is more susceptible to noise in the data (Phillips, 2000). From empirical observations during this study, these two methods are not reliable for sources deeper than about 500 ft (150 m).

Anomaly Separation by Matched filtering

Anomaly separation by matched filtering allows qualitative examination of shallow versus deep character of the aeromagnetic data across the area. Matched filtering was used to separate the aeromagnetic data into several depth components, based on analytical comparisons to the magnetic effects of layers of hypothetical sources at different depths (Syberg, 1972; Phillips, 2001). The data were separated into four components (Fig. 2), corresponding to source layers at depths of 0.4 km (1300 ft), 2.0 km (6600 ft), 6 km (19,700 ft), and 20 km (12.5 miles). The layer depths can be used to estimate the maximum depths of sources represented by each component (Phillips, 2001). Although the data were separated into four components, there is considerable overlap between components. The overlap indicates sources extend over a wide range of depths or there are laterally extensive sources at shallow depths that produce broad anomalies, which masquerade as deeper anomalies.

PROFILE MODELS

Preliminary work with the aeromagnetic data revealed large uncertainties in the results for the region surrounding Santa Fe and north of Interstate 25 (Plate 1). Depth estimates ranged widely, even near each other, likely representing separate magnetic sources at different depths. In particular, it was difficult to determine if several elongated, subtle, north-south, sinuous anomalies just north of Santa Fe were related to basement rocks or to magnetic rocks above the basement. These anomalies are most apparent in the matched-filtered component showing anomalies due to the shallowest sources (Fig. 2a). To resolve these problems, we developed geophysical models along several profiles in this region (located on Fig. 1 and Plate 1) that incorporated gravity data, and other geophysical and geologic constraints.

Model Constraints

Four profiles were extracted from a map of isostatic residual gravity data (Fig. 3) and the reduced-to-pole aeromagnetic data (Plate 1) for modeling. The profiles were chosen to cross aeromagnetic anomalies of interest and lie next to as many gravity stations as possible (Fig. 3), for better data control. To aid in the modeling, low-resolution aeromagnetic data were extracted from the regional compilation developed by Sweeney and others (2002) for the east sides of the profiles, where the profiles were located outside the high-resolution aeromagnetic survey area.

The isostatic residual gravity data are from Gillespie and others (2000). These data were produced by removing a regional field based on an isostatic model to focus on gravity anomalies in the upper crust. Isostatic residual gravity data in this area are most sensitive to the contrast in density between the bedrock and poorly consolidated sediments (Grauch and others, 1999), so they provide an important constraint on the general configuration of the basin floor.

Geologic constraints were provided by the Yates La Mesa #2 well and geologic cross-sections developed for Tesuque (Borchert and Read, 1998), Horcado Ranch (Koning and Maldonado, 2001, revised January 2003), and Turquoise Hill (Koning and Hallett, 2000) 7-1/2-minute quadrangles. Limited additional constraints were developed from proprietary seismic-reflection data provided by the SAGE group (J. Ferguson, Summer of Applied Geophysical Experience).

We began by constructing a model along the "Tesuque profile" (Fig. 1), which provided a starting constraint for the other three profile models. This profile matches the location of a geophysical model developed by Biehler and others (1991), which incorporates results from gravity, seismic-refraction, and magnetotelluric surveys (they showed magnetic data but did not attempt a fit). We relied on the constraints provided by their seismic refraction results (Fig. 4a), densities from borehole logs located primarily in the Albuquerque basin (Birch, 1982 and our own examinations), limited magnetic susceptibility field measurements, and geologic concepts. The primary geologic concept guiding model development, which differs from previous ideas, was provided by D. Koning (personal commun., 2003). Based on examination of cuttings from the Yates La Mesa #2 well, geologic mapping, and inspection of the SAGE proprietary seismic reflection data, Koning expects that Oligocene volcanic rocks in this area rest on the eroded basal portion of the Paleozoic section or directly on Precambrian basement. Although our model cannot distinguish the Paleozoic rocks from the basement at depth (Fig. 4a), a major consequence of this concept is a thick section of Santa Fe Group overlying the Oligocene volcanic rocks, which can be constrained by the gravity data. This thick section is difficult to represent as one model layer due to expected increases in density with depth due to compaction. Therefore, we used two layers to represent the Santa Fe Group that are based on a density-depth function that fits observations from borehole density logs and coincides with the variations in seismic velocities from Biehler and others (1991) (Fig. 4a, Table 1). The final model for the Tesuque profile (Fig. 4a) provided the basic concept and parameters for the models along the other three profiles (Figs. 4b-d).

Table 1 describes the relations of the elements of the models to geologic units and gives explanations for how the density and magnetic properties of the units were chosen. Note that model units are based mainly on general differences in lithology. The corresponding ages and geologic unit names are given to help put the model into geologic context and are subject to re-interpretation. Except for the magnetization of the Precambrian basement rocks, these physical properties remained constant for all models. The variations in magnetization of the basement rocks are required by the modeling and are evident from interpretation of the maps (Fig. 5).

Results of Interpretation

The models provide general guides on the depths to basement and the thickness of the Santa Fe Group aquifer (Fig. 4). They were used to guide the contoured representations of depths to Precambrian basement rocks (Fig. 5) and to Oligocene volcanic rocks (Fig. 6). Detailed results are discussed within the following sections on the different geologic units. The main results are as follows.

- The basement surface generally dips 5-20^{o} to the west from the mountain front, reaching depths greater than 7000 ft west and north of Santa Fe.

- Several north-south trending, elongated aeromagnetic anomalies northwest of Santa Fe are interpreted as narrow structural highs that involve Precambrian through Oligocene rocks (Figs 4b and c), Alternatively, these structural highs may also be associated with local intrusions, probably related to Oligocene magmatic activity. In the alternate model, basement relief would be minimal, and the shallow magnetic source required by the data would be represented by paleotopographic relief on an intrusion rather than by structural relief. In both cases, the models imply that the Santa Fe Group thins to less than 2000 ft in the areas corresponding to the elongate anomalies.

- West and northwest of the inferred, elongated structural highs, the Santa Fe Group generally thickens to greater than 7000' (2134 m) under the eastern edge of the Cerros del Rio volcanic field.

- The gravity data combined with other model constraints for Profile 3 (Fig. 4d) require a westward thickening, moderately low-density wedge of undifferentiated sedimentary rocks on the west side. This wedge may be dominantly Galisteo Formation or Mesozoic rocks, based on the range of densities expected for these units.

Limitations of Results

The geophysical models are designed to focus on the main features of the data and are inherently somewhat ambiguous. As a consequence, fits to the details of the data curves have not been attempted, especially for the gravity data, which has poor data control in local areas along the profiles (Fig. 3). Magnetic data over the extreme eastern and western ends of the profiles were not required to fit well for several reasons: (1) variable magnetic rocks (basalts and Precambrian basement rocks) are exposed at the surface and therefore insignificant variations in magnetization and topography are overemphasized; (2) sources off the ends of or to one side of the profiles may have an effect but are hard to represent properly; and (3) regional magnetic data extracted for the western ends of the profiles have poor resolution.

Simplifying assumptions about physical properties and the general thicknesses of units are required to minimize the number of variables to model, but also produce results that should be used as general guides and not applied to problems at local scales. Moreover, alternative models could be constructed to fit the same data. In particular, structural relief and variations in thickness of units could be alternatively modeled as variations in physical properties. However, this ambiguity has been minimized in these models due to the independent constraints. The largest ambiguities are likely to affect the thickness and configuration of the Oligocene volcanic section, because these rocks are known to have considerable variability in lithology and physical properties (Kautz and others, 1981; Smith and others, 1991). Specific uncertainties in the model results are listed below.

- Steep dips on the basement surface could alternatively be modeled using faults or series of faults with offsets less than about 1000' (300 m).

- The interface between the basement rocks and the overlying rocks is poorly constrained, especially on the west, where this interface is much deeper. We estimate the error in depth may be as much as 30% of the modeled depth.

- As mentioned above, the small-scale structural highs modeled for the basement through Oligocene section may be produced by a combination of structures and igneous intrusions. A structural origin of some sort is supported by the steep magnetic gradients associated with the corresponding elongated aeromagnetic anomalies (see the section on shallow faults) and by the presence of horsts, grabens, and anticlines of similar orientation and scale exposed in basement rocks to the east (Kelley, 1978).

- The terminations of the undifferentiated sedimentary rocks and Oligocene rocks are poorly constrained. Interfingering between units cannot be resolved.

- The boundaries shown between Precambrian rocks of different properties may not represent petrologic boundaries. The variations in magnetic properties are likely much more variable and gradational.

Finally, the configuration of the modeled units may be affected by three-dimensional variations that occur off the profile. This problem is most evident in profile 2, which crosses the aeromagnetic map near the transition from a large broad magnetic high on the north to only subtle features on the south (Plate 1). The effect of the magnetic high on the north required the addition of magnetic source at depth in the model (Fig. 4c) that likely does not represent a real source.

PRECAMBRIAN BASEMENT

Hydrogeologic Significance: Fractured, locally cavernous Mississippian-Pennsylvanian marine limestones unconformably overlie Precambrian basement rocks, except where they were eroded after Laramide time (Kelley, 1977; 1978). Water wells tapping the limestones and fractured Precambrian rock are productive and show that the basement unconformity has hundreds of feet of relief over short distances (J. Hawley, written communication, 2000). Nevertheless, depth estimates to Precambrian basement can provide general guides for locating drill holes.

Expected Magnetic Expression: Northeast of the Eldorado subdivision (Fig. 1), Precambrian basement rocks include amphibolite, biotite gneiss, and granitic rocks (Read and others, 1999). Measured magnetic susceptibilities do not have a simple correspondence to mapped rock units. Rocks range from weakly magnetic (average susceptibility of 0.0008 SI) to very magnetic (susceptibilities >0.01) (V.J.S. Grauch and M. Hudson, unpub. magnetic susceptibility measurements, 1999, and 2002, respectively). The most magnetic basement rocks may be the main source of broad magnetic highs in the eastern part of the Eldorado subdivision, north and south of Santa Fe along the western front of the Sangre de Cristo Mountains, and near Española (cf. Plate 1 and Fig. 5). They are similar to the Sandia granite east of Albuquerque (Kelley, 1977) in expression on aeromagnetic maps (Grauch, 1999).

Methods of Interpretation: Depths were determined from the geophysical profile models (Fig. 4) and from depth estimation along profiles in other areas using primarily multi-source Werner (Hansen and Simmonds, 1993), Euler deconvolution (Thompson, 1982), local wave-number or source parameter imaging (Thurston and Smith, 1997; Smith and others, 1998), and analytic signal (Nabighian, 1972; 1974) methods in the computer program PDEPTH (Phillips,

1997). Comparisons with the results of the horizontal-gradient (Roest and Pilkington, 1993; Phillips, 2000) and autocorrelation (Phillips, 1979) methods were helpful. From model tests and results on the actual data, the multi-source Werner and Euler deconvolution methods gave the most reliable results for estimating depths to the magnetic Precambrian basement. The local wave-number method worked well for shallow basement depths in the Eldorado area. Matched filtering results (Fig. 2) were used to qualitatively assess the range of depths of the basement-related anomalies.

Results of Interpretation: Depth estimates to magnetic Precambrian basement over most of the basement-related anomalies (Fig. 5) are greater than 3000 ft (914 m). In the northeast part of the Eldorado subdivision, basement rises to the surface (Fig. 1). In this area the estimates could be only generally contoured (Plate 2). These depth contours show that the basement is dipping 15^{o} overall to the southwest (comparable to the 12^{o} hypothesized by Biehler, 1999) and plunging more steeply to the southeast. Although not evident from the depth contours, the Seton Village fault of Spiegel and Baldwin (1963) can be extended through this area (Plate 2), based on the location of maximum horizontal-gradient magnitudes.

A major contrast in magnetic lithology likely produces the southern termination of the broad magnetic anomaly north of Santa Fe (M, Fig. 5). The termination is interpreted as a contrast in rock type between magnetic Precambrian basement on the north and weakly magnetic Precambrian basement on the south rather than as structural relief. This interpretation is based primarily on gravity data from the area that do not show a change in the north-south orientation of contours near 106^{o}W longitude between 35^{o}37'30"N and 35^{o}45'N (Fig. 3). The geophysical profile models, which are discussed in detail in a previous section, support the interpretation (Fig. 4). The contrast in magnetic lithology may have originated as an intrusive contact or a pre-Tertiary fault.

Depth contours were constructed from the profile models west and northwest of Santa Fe (Fig. 5). The contours are dashed where depths are poorly constrained, primarily where the modeled basement is not very magnetic (PC/Madera unit on Fig. 4). In addition, the fairly narrow structural highs involving the Precambrian basement in models for Profiles 1 and 2 (Figs. 4b and 4c) can be alternately modeled as Tertiary intrusions, as discussed in the section on profile models. This alternate model would likely give a more consistent and gradual slope for the Precambrian surface (Fig. 5).

Limitations of Results: In addition to the standard limitations of depth estimation techniques, variations in the magnetic properties of the Precambrian basement rocks place an important limitation on the depth-estimation and geophysical model results. Where large volumes of weakly magnetic Precambrian basement are present, aeromagnetic depth-estimation methods will not be effective. Estimated depths are also insensitive to local variations in basement relief. Variability in both basement rock type and in basement relief are evident from wells drilled in the Eldorado area (J. Hawley, written commun., 2000; Biehler, 1999). The magnetic depth estimations in this area can only provide a regional view of the basement configuration at depth.

Recommendations for Future Work: Deep-looking electrical methods, seismic-reflection data, and better coverage of gravity data would help constrain depth to basement in the areas that cannot be resolved by the magnetic data.

TERTIARY INTRUSIVE ROCKS AND VOLCANIC VENTS

Hydrogeologic Significance: Intrusive bodies at depth render drilling difficult and may impart metals or other toxic elements to the groundwater. Dikes and sills emanating from the bodies may degrade adjacent aquifers. The presence of large intrusive bodies may also indicate that fractures are the dominant control on ground-water flow.

Expected Magnetic Expression: The Cerrillos intrusion (Fig. 6) at the Cerrillos Hills (Fig. 1) is associated with a strong positive magnetic anomaly in this data set (Plate 1) and on regional magnetic maps (Cordell, 1984). Associated outliers are also expected to produce strong, positive anomalies. One small Tertiary intrusion exposed northwest of the Transocean McKee well (Fig. 6) is associated with a subtle magnetic high (Plate 1).

Smaller intrusions that served as vents for volcanoes or cinder cones are commonly associated with local, circular, high-amplitude magnetic anomalies, generally less than a mile (1.6 km) in diameter, that can be either positive or negative. Examples of these circular magnetic anomalies are abundant in the central to northern part of the Cerros del Rio volcanic field (cf. Fig. 1 and Plate 1) and within volcanic fields south of Albuquerque (Grauch, 1999). Similar, moderate-amplitude negative circular anomalies commonly occur within mapped or interpreted Oligocene volcanic rocks (Plate 1; see next section), but none are associated with exposed intrusions (A. Lisenbee, written commun., 2001). The negative magnetic signature indicates a volcanic or shallow-intrusive origin (Grauch and others, 1997) with substantial depth extent, but whether there is associated extrusive material is not known. These features, called volcanic vents(?) for convenience, are considered to be associated with Oligocene magmatic activity based on similar depths to the more horizontally layered Oligocene volcanic rocks (Plate 2).

Methods of Interpretation: Lateral extents of Cerrillos intrusive rocks and volcanic vents(?) near the edges or outside of the Cerros del Rio volcanic field are outlined (Fig. 6) using the local maxima of horizontal-gradient magnitudes (Cordell and Grauch, 1985; Blakely and Simpson, 1986). There are so many vents within the central part of Cerros del Rio volcanic field that they are outlined collectively (Fig. 6).

Estimates of the depths to each inferred intrusion were determined from profiles using primarily multi-source Werner (Hansen and Simmonds, 1993), Euler deconvolution (Thompson, 1982), local wave-number (Thurston and Smith, 1997; Smith and others, 1998), analytic signal (Nabighian, 1972; 1974), and horizontal-gradient (Roest and Pilkington, 1993; Phillips, 2000) methods in the computer program PDEPTH (Phillips and Grauch, in press). The depth estimates were commonly somewhat variable across the anomaly, so depth ranges rather than a single depth were inferred (Plate 2).

Results of Interpretation: The Cerrillos intrusion includes a wide area surrounding the Cerrillos Hills (Figs. 1 and 6). Steep magnetic gradients on all but the western side of the broad

anomaly suggest that the intrusion has near-vertical contacts for most of its perimeter, despite its laccolithic nature apparent from geologic mapping (Grant, 1999; Maynard and Lisenbee, in press). This suggests the laccolithic sills are generally thin on most sides of the intrusion, or most abundant at depth on the western side.

Depth estimates show variable, but fairly shallow depths to the Cerrillos intrusion. The roots of the intrusion extend to great depths, as indicated by its expression in all anomaly components (Fig. 2). It is difficult to magnetically distinguish Cerrillos-related intrusive rocks and Oligocene volcanic rocks near La Cienega (Plate 1) and near the Cerrillos intrusion, where the intrusion is overlain by the volcanic rocks (Kelley, 1978; Fig. 7).

The negative anomalies with circular outlines at Buckman Mesa and to the south, near Caja del Rio canyon, are associated with exposed volcanic vents of Pliocene-Quaternary age (Plates 1 and 2). The irregularly shaped outlines north of the Cerrillos intrusion are likely related to the intrusion, because they are associated with high-amplitude positive anomalies and exposures of related intrusive rocks (Fig. 6). The rest of the generally circular outlines away from the Cerrillos Hills and La Cienega areas on Figure 6 are associated with negative anomalies and are interpreted as isolated volcanic vents(?), likely affiliated with Oligocene magmatic activity. Ranges of depth estimates for these inferred Oligocene volcanic vents(?) fit within the ranges of depth estimates for buried, inferred Oligocene volcanic rocks (Plate 2). Lack of exposure of these vents(?) prevents examination of their geologic origin.

Limitations of Results: Although the main parts of the intrusive bodies are well defined in the aeromagnetic data, dikes and sills that emanate from them are not. Thus, the sphere of influence of each intrusion may be much wider than indicated. The volcanic vents(?) may also have influence away from their primary magnetic expression. The Yates La Mesa #3 well encountered many dikes and sills within the volcaniclastic Espinaso Formation (Grant, 1999; Koning and Hallett, 2000). These may be related to any of several interpreted volcanic vents(?) located nearby (Fig. 6).

Recommendations for Future Work: Drilling or detailed ground-based electrical geophysical studies may help delineate the sphere of influence of the intrusions and volcanic vents(?). Geochemical studies of water and cuttings from nearby wells may indicate the chemical influence of these rock types on water quality.

OLIGOCENE VOLCANIC ROCKS

Hydrogeologic Significance: Oligocene volcanic rocks consist of the predominantly volcaniclastic Espinaso Formation (Kautz and others, 1981) and overlying Cieneguilla basaltic rocks (Sun and Baldwin, 1958; Koning and Hallett, 2000; Sawyer and others, 2002). The Cieneguilla rocks are primarily located in the vicinity of La Cienega. In this area, brecciated lava flows dominate the lithology of the Espinaso Formation (Koning and Hallett, 2000; Sawyer and others, 2002). In the southern half of the study area, these units directly underlie aquifers of the Santa Fe Group (Tesuque and Ancha Formations), so depth estimates to the Oligocene volcanic rocks help assess potential aquifer thickness. In a few places, the Oligocene volcanic rocks are absent from the section, resulting in Santa Fe Group resting directly on older sedimentary units, such as the clastic Galisteo Formation of Eocene age or a variety of

sedimentary lithologies of Mesozoic age (Kelley, 1978; Koning and Hallett, 2000). The Oligocene volcanic rocks make drilling difficult and have much lower permeability than the sedimentary units (Spiegel and Baldwin, 1963). Water yields depend on fracturing and clastic interbeds. In addition, volcanic rocks may impart metals or other toxic elements to the groundwater. Therefore, prediction of their presence or absence at shallow depths is important for planning water well locations.

Expected Magnetic Expression: Where exposed southeast of the Cerrillos intrusion, the Espinaso Formation corresponds to a distinctive, mottled pattern on the aeromagnetic map (cf. Fig. 7 and Plate 1). Measurements of magnetic susceptibility on a few typical hand samples (provided by G. Smith at University of New Mexico, 1999) give high values (0.01-0.03 SI). Cieneguilla rocks are likely even more magnetic, because outcrops correspond to high-amplitude magnetic anomalies near La Cienega (Plate 1). Aeromagnetic patterns associated with Cieneguilla rocks and perhaps also late Espinaso Formation (Koning and Hallett, 2000; Sawyer and others, 2002) appear as a collection of individual, elongated anomalies, oriented primarily northeast, from La Cienega, to the Yates La Mesa #3 well, to the northern part of the Eldorado subdivision (Plate 1). This pattern may indicate basalt flows restricted to paleochannels.

Methods of Interpretation: Examination of aeromagnetic patterns provided guides for outlining the lateral extent of the Oligocene volcanic rocks. Inspecting the patterns in conjunction with geologic mapping (Kelley, 1978, Lisenbee, 1999; Koning and Hallett, 2000) allowed inferences about aquifer units at depth. Depth estimates were determined using both profile-based and grid-based methods as well as the geophysical models (Fig. 4). Profile-based depth-estimation methods used were primarily multi-source Werner (Hansen and Simmonds, 1993), Euler deconvolution (Thompson, 1982), local wave-number (Thurston and Smith, 1997; Smith and others, 1998), analytic signal (Nabighian, 1972; 1974), and horizontal-gradient (Roest and Pilkington, 1993; Phillips, 2000) methods in the computer program PDEPTH (Phillips, 1997; Phillips and Grauch, in press). The grid-based methods (horizontal-gradient and local wave-number methods, implemented by Phillips, 2000) were most useful for determining the shallowest depths.

Results of Interpretation: In the southern part of the study area, most of the lateral limits of the Oligocene volcanic rocks could be determined from the termination of aeromagnetic patterns (Plates 1 and 2). However, the northern limit of the volcanic rocks cannot be recognized due to the deeper levels of the units. The Oligocene volcanic rocks could not be magnetically distinguished from the Cerrillos intrusion and the Cerros del Rio volcanic field along parts of their western limit (Fig. 7). Although the age and affiliation is unclear, the magnetic data indicate igneous rocks are shallow and abundant in the Cerrillos Hills.

The high-amplitude elongate-anomaly patterns of the younger Cieneguilla basaltic rocks (or possibly flows within the Espinaso Formation) do not extend much further south than the Yates La Mesa #3 well (Plate 1). The mottled aeromagnetic signature of the volcaniclastic Espinaso Formation prevails in the southern part of the area (cf. Fig. 7, Plate 1) under widespread cover of Ancha Formation, which is commonly considered to be the upper part of the Santa Fe Group (Spiegel and Baldwin, 1963; Koning and others, 2002). The surface of the volcanic rocks is eroded where exposed on the south (Smith and others, 1991) and where penetrated by shallow water wells (Koning and Hallett, 2000), implying that it could be quite

irregular under cover. At the most southern end of the area of Oligocene volcanic rocks, the mismatches between the interpreted lateral limits and the mapped contacts of Espinaso Formation (Fig. 7) indicate improvements to the regional geologic map (Kelley, 1978) are required. The mapped contacts from more recent, detailed mapping (Lisenbee, 1999; Maynard and Lisenbee, in press) show excellent correspondence.

The magnetic expression of Oligocene volcaniclastic rocks is notably absent in three large areas, where Ancha Formation likely rests directly on older sedimentary rocks (Plate 2, A1-A3). In the area (A1) along the western limit of Oligocene volcanic rocks north of the Cerrillos intrusion, Ancha Formation may overlie Mesozoic sedimentary rocks on the west and the Eocene clastic Galisteo Formation on the east, based on geologic relationships and subsurface data from the Gianardi #1 CKZ well (Koning and Hallett, 2000). Further to the west, in between inferred Cerrillos-related intrusions, the underlying geologic unit is unclear. The magnetic signature (Plate 1) suggests that the Oligocene volcanic rocks may be present at some depth, but no definitive results could be obtained from depth estimation methods.

In the second area (A2), recessed into the region of volcanic rocks just southeast of 35°30'N, 106°W, Ancha Formation likely overlies west-dipping Galisteo Formation, based on geologic relations nearby (Lisenbee, 1999). The east side of this area (A2) is defined by a down-to-the-east fault (F3, Plate 2). Where the fault is exposed south of A2, it juxtaposes different strata within the Galisteo Formation (Lisenbee, 1999). To the north, where the fault is not exposed, the magnetic patterns indicate Oligocene volcanic rocks are also involved in the faulting; they are down-dropped on the east against Galisteo Formation on the west. In contrast, the western side of this area is defined by the eroded termination of west-dipping Espinaso Formation, as inferred from geologic strikes and dips (Plate 2; Lisenbee, 1999). Linear magnetic anomalies parallel to this and other erosional contacts of Espinaso Formation in the area (Plate 2) indicate that the uppermost Galisteo Formation contains strata that are somewhat magnetic. These anomalies are most apparent from the shallowest anomaly component (Fig. 2a).

Pre-Ancha rocks in the third area (A3) between the eastern limit of Oligocene volcanic rocks and outcrops of Precambrian are structurally complicated (Lisenbee, 1999). From comparing mapped geologic units south of the area, Ancha Formation likely overlies Galisteo Formation near the eastern limit of Oligocene rocks, Mesozoic units further to the east and south, and Paleozoic rocks close to the shallow portions of the Precambrian (Plate 2). On the other hand, one can follow the signature of the magnetic layers in the uppermost Galisteo Formation into this area, suggesting that the subtle, mottled signature of the shallowest depth component over most of the area (Fig. 2a) is associated with upper Galisteo Formation. Alternatively, the mottled pattern may be due to recent magnetic detritus shed from the Precambrian exposures to the east or buildings in the area.

Contours of depth estimates to the Oligocene volcanic rocks (Plate 2) were drawn from the results of depth-estimation methods for depths >1000 ft (330 m) and from the geophysical profile models (Fig. 4) for deeper levels. Based on similarities between estimated depths to the volcanic vents(?) and those to the Oligocene volcanic rocks in many areas, it is assumed that the rocks are contemporaneous and spatially related. Thus, the depths to these volcanic vents(?) were used to help interpret contours.

The depth estimates indicate that Oligocene volcanic rocks are shallow (<250 ft; <75 m) under most of their extent in the southern part of the area (pink shading, Plate 2), within the Santa Fe embayment (Kelley, 1978). The rocks dip into the Española basin on the north as an asymmetric syncline (Plate 2; Fig. 6). The western limb of the syncline continues under the Cerros del Rio volcanic field and likely wraps around the northern end of the Cerrillos uplift (Sawyer and others, 1999), represented by the large gravity high surrounding the Cerrillos intrusion (cf. Figs. 3 and 6). The eastern limb generally parallels the mountain front. The volcanics terminate near or against basement rocks along the eastern limb (Fig. 4), but where this occurs is not well constrained. The volcanic rocks likely interfinger with older Santa Fe Group sediments, as observed in outcrop by Smith (2000). As discussed in connection with the geophysical profile models, Oligocene volcanic rocks are disrupted within several structural highs on the basement that trend north-south northwest of Santa Fe (Figs. 4 and 7; Plate 2), which may have involved Oligocene intrusive activity as well.

Strike and dip measurements from isolated exposures of the Espinaso Formation (Plate 2), together with the aeromagnetic interpretations, suggest that the Espinaso Formation thins to its eastern termination in and southwest of the Eldorado subdivision. Based on the depth contours, the dip may steepen considerably along this eastern edge from the measured 14^{o} dip near F3 on the south to Eldorado on the northeast (Plate 2).

The depth estimates indicate several isolated depressions in the surface of the Oligocene volcanic rocks near Eldorado and east of the Cerrillos intrusion (Plate 2), which have no expression in surface rocks. These depressions likely indicate significant thickening of the overlying Ancha Formation. The elongated depression northeast of Eldorado, which reaches depths of nearly 1000 ft (330 m), may be related to the eastern limb of the larger syncline formed in the Oligocene volcanic rocks (Plate 2).

Limitations of Results: The depth estimation methods used can only resolve the general form of irregularities on the Oligocene volcanic surface (Plate 2), due to interference from neighboring sources and unknown variations in magnetization. Moreover, the methods inherently provide results only for the shallowest magnetic sources and do not resolve the depths in between sources, where volcanic rocks may be missing or at much greater depths. Thus, in between the elongated anomalies of the flow-like pattern, there may be greater accumulations of Ancha Formation than are indicated or could be resolved by this study.

Recommendations for Future Work: Improved magnetic depth estimation methods, detailed ground-based electrical geophysical measurements, or shallow seismic-reflection data acquisition may give better resolution of local variations in the depths to volcanic rocks in selected areas. Combining water level information from wells with the depth information can give estimates of thickness of the saturated Santa Fe Group section. In the Eldorado area where Oligocene volcanic rocks are absent (A3, Plate 2), subsurface interpretations using well data could help predict the sedimentary sequence below the Ancha Formation. Ground magnetic profiles and rock property measurements in the eastern part of the Eldorado subdivision may help resolve the source of the subtle, mottled magnetic signature. Geochemical studies of water and cuttings from wells that penetrate the volcanic rocks may indicate the chemical influence of these rock types on water quality.

PLIOCENE-QUATERNARY VOLCANIC ROCKS

Hydrogeologic Significance: Pliocene-Quaternary volcanic rocks in the study area include the basalts of the Cerros del Rio volcanic field (Fig. 1) and the Jemez volcanics, the silicic volcanic rocks that erupted from the Jemez Mountains volcanic field, west of the study area (Fig. 7; Kelley, 1978; Bailey and others, 1969). These volcanic rocks overlie the Tesuque Formation of the Santa Fe Group, the main aquifer of the Santa Fe area (Lewis and West, 1995). West of the Rio Grande, the Puye Formation, an aquifer for the Los Alamos area, lies between the Tesuque Formation and the Pliocene-Quaternary volcanic rocks (Lewis and West, 1995; Kelley, 1978). East of the river, the Ancha Formation overlies the Tesuque Formation, and is interbedded with the Cerros del Rio basaltic lava flows (Koning and Hallett, 2000; Koning and others, 2002). Thus, the bulk of the Santa Fe Group aquifers lie beneath the Pliocene-Quaternary volcanic rocks, which gives importance to knowing the lateral extent and thickness of the volcanic rocks. In particular, the Cerros del Rio basalts can be fairly thin at the margins of the field (20-100 ft; Sun and Baldwin, 1958; Thompson and others, 1997). In these areas they may have some affect on recharge and water quality, but little affect on ground-water flow. In addition, knowing if volcanic rocks underlie the Ancha Formation helps identify potentially difficult drilling sites and places where metals or other toxic elements may enter the ground water.

Expected Magnetic Expression: Where exposed, the Cerros del Rio basaltic rocks are very magnetic, evidenced by the high-amplitude negative and positive magnetic anomalies that correlate with topographic contours (Grauch, 1987) and mapped flow contacts (Sawyer and others, 2002). Paleomagnetic and rock-property measurements (M. Hudson and M. Hopkins, unpub. data, 2000) indicate that the magnetizations of these rocks are generally dominated by strong remanent (permanent) magnetization having both normal and reversed orientations with respect to the present Earth's magnetic field, depending on the age of formation. The normal and reversed orientations give rise to the positive and negative anomalies, respectively.

The Bandelier Tuff represents exposures of Jemez volcanic rocks in the study area. Northwest of Buckman Mesa, it has little to no aeromagnetic expression (Fig. 7). However, west of Cochiti Pueblo it is associated with moderate-amplitude negative anomalies (Sawyer and others, 2002). Where the Bandelier Tuff overlies the Cerros del Rio volcanic rocks along the west side of the Rio Grande (Fig. 7), the signature of the Cerros del Rio rocks dominate the aeromagnetic map (Plate 1).

Methods of Interpretation: Lateral extent of the Cerros del Rio volcanic field was outlined (Figs. 6, 7, Plate 2) based on visual inspection of the aeromagnetic patterns and using the local maxima of horizontal-gradient magnitudes to determine the edges (Cordell and Grauch, 1985; Blakely and Simpson, 1986). Comparisons between the results of the local wave-number method (Thurston and Smith, 1997) and grid-based horizontal-gradient method applied to both reduced-to-pole magnetic data and pseudogravity (Phillips, 2000) allowed qualitative determination of where basaltic rocks were generally thin (less than 150 ft or 50 m?). Thin basalt was interpreted where both the local wave-number method gave sheet solutions and where the depth estimates from the two different applications of the horizontal-gradient method were close (Grauch and others, 2001).

Results of Interpretation: The aeromagnetically determined, lateral extents of the Cerros del Rio volcanic field closely approximate geologically mapped contacts (Fig. 6). Slight discrepancies are evident along the southern margin of the field and directly west of the Yates La Mesa #2 well. The aeromagnetically determined southern limit is located 1500-2000 ft (450-600 m) away from the mapped contact, within the area of mapped Ancha Formation. This discrepancy is confirmed by detailed mapping (Sawyer and others, 2002), indicating that the Ancha Formation covers the volcanic rocks along this margin.

Outside of the area interpreted as having widespread volcanic vents (Fig. 6), the basaltic rocks have anomaly patterns that are more subdued and lower in amplitude, indicating the basaltic rocks are probably not as thick as in the vent area. Thin basalt could be qualitatively determined surrounding the intrusion at Buckman Mesa, consistent with mapping by Dethier (1997), and in several places along the margin of the volcanic field (Plate 2).

Limitations of Results: In some places, the lateral limits of the Cerros del Rio volcanic field are difficult to distinguish from adjacent magnetic igneous (Fig. 7). Due to likely large variations in magnetic properties, the difference in aeromagnetic character used to make qualitative inferences about thickness of the basaltic rocks may not hold up in certain areas. Even at the margins of the volcanic field, the aeromagnetic data give little quantitative information about the thickness of the basaltic rocks.

Recommendations for Future Work: Within the volcanic field, thickness of the basaltic rocks on top of Santa Fe Group may be determined by ground-based electrical geophysical methods or deep-looking seismic reflection methods. Deep-looking electrical geophysical methods (magnetotelluric methods) have been successful in ascertaining depth to conductive Mesozoic shales (such as the Mancos shale) underneath basalts of the Cerros del Rio volcanic field (Sawyer and others, 1999). Locating the buried extent this unit at depth would also give constraints on the thickness of Santa Fe Group underneath the basalts. Geochemical studies of water and cuttings from wells that penetrate the volcanic rocks may indicate the chemical influence of these rock types on water quality.

SANTA FE GROUP

Hydrogeologic Significance: The Santa Fe Group includes the main aquifers in the basin. Where Santa Fe Group sediments are predominantly coarse-grained (sand), the aquifer may be the most productive. Knowledge of overall sediment thickness is important for understanding ground water storage and developing ground water flow models. Depth estimates to Oligocene volcanics, discussed previously, can be used to determine the thickness of the overlying Santa Fe Group.

Expected Magnetic Expression: Santa Fe Group sediments in the Albuquerque basin produce weak to moderate aeromagnetic anomalies where they are juxtaposed at faults and where they compose irregular topography (Grauch and others, 2001). The sediments have magnetic susceptibilities that generally fall between 0.0002 and 0.005 SI, with larger values corresponding to fractions with coarser grain size; these values are large enough to produce weak to moderate aeromagnetic anomalies (Hudson and others, 1999).

Methods of Interpretation: Inspection of the topographic, geologic, and aeromagnetic maps for correlations and relations between units and aeromagnetic signature allow interpretation of areas of magnetic Santa Fe Group that are inferred to represent coarse grain size.

Results of Interpretation: The thickness of the Santa Fe Group can be determined from the depths to the Oligocene volcanics in much of the study area, as discussed above.

In San Ildefonso Pueblo (Fig. 1), magnetic anomalies correlate better with hills composed of Puye Formation (Kelley, 1978) than with local exposures of overlying Bandelier tuff, indicating that the Puye Formation is moderately magnetic and the source of the magnetic anomalies (Fig. 7, Plate 2). The coarse-grained lithology of the Puye Formation (Manley, 1979; Koning and others, 2002) supports the inference that coarser grained Santa Fe Group is more magnetic.

Correlation of subtle aeromagnetic anomalies and topography is also evident in an area generally located east of the Cerros del Rio volcanic field between Pojoaque and the Yates La Mesa #2 well (Plate 2). This magnetic character generally corresponds to the coarse upper unit of Tesuque Formation mapped in the area, which is generally composed of sand and gravel (unit Ttap2 of Koning, 2002; unit Tta3 of Koning and Maldonado, 2001). Similar areas, also interpreted as Santa Fe Group dominated by coarse-grained fraction, are located about 6 miles (10 km) north of Santa Fe and northeast of the Santa Cruz River (Fig. 7, Plate 2). However, it is unclear whether these coarse-grained facies extend below the water table.

Limitations of Results: Limitations on estimates of the thickness of the Santa Fe Group were previously discussed relative to the depth estimates of the Oligocene volcanics.

Interpretation of areas of coarse-grain sizes in the Santa Fe Group are based on a general correlation observed between magnetic properties and grain size from the Albuquerque basin (Hudson and others, 1999), which has not been tested in the Española basin.

Recommendations for Future Work: Examination of lithologic properties of cuttings from water wells, as well as magnetic susceptibility measurements in bore holes should help to better establish a relation between magnetic properties and grain size in Santa Fe Group sediments.

SHALLOW FAULTS

Hydrogeologic Significance: Faults that juxtapose units of different lithology within the Santa Fe Group serve to partition aquifers and themselves can be significant barriers to or conduits of fluid flow themselves (Haneburg, 1996).

Expected Magnetic Expression: Faults that juxtapose Santa Fe Group units of differing magnetic properties in the Albuquerque basin are generally expressed as linear anomalies on aeromagnetic maps, with considerable variation in detail (Grauch and others, 2001). Associated anomaly amplitudes in the Albuquerque basin typically range from 2 to 10 nanoTeslas. Linear anomalies associated with faults in the Santa Fe Group of the Española basin are generally

similar, but have amplitudes at the low side of this range and are harder to distinguish from solely topographic effects. Faults within more magnetic units, such as the Oligocene volcanic rocks, also appear linear, but are much more striking on the aeromagnetic map (Plate 1), because they have higher amplitudes (cf. F1-F5, Plates 1 and 2).

Methods of Interpretation: Because of the focus on shallow faulting, the shallowest depth component from the anomaly separation (Fig. 2a) was used to interpret faults. The data from this component, its computed horizontal-gradient magnitudes, and topography were inspected together for the interpretation. Alignments of maxima of horizontal-gradient magnitudes provided location information. Because not all maxima are related to faults, criteria were established to help distinguish gradients related to faults versus those related to unfaulted contacts or due solely to topography. First, only linear or extensive semi-linear gradients were considered; this eliminates gradients produced by abrupt changes in magnetization within one rock unit. Second, gradients were compared to topographic slopes. Where they corresponded, the magnitudes of the gradient and the topographic relief were inspected to judge whether the topographic slope alone could cause the gradients. High-magnitude gradients corresponding to moderate to low topographic relief indicate that a magnetization contrast in addition to the topographic slope must be present. Interpreting these gradients as faults, even though they coincide with topographic slopes, is reasonable because faulting commonly controls topography. These gradients were interpreted as faults because topography commonly correlates with faults. Finally, multiple gradients were inspected in relation to topography and geology to determine if they were produced by one or multiple faults. Multiple gradients can be associated with single faults that juxtapose shallow thin magnetic units against deep thick magnetic units (the thin-thick layers model of Grauch and others, 2001).

Results of Interpretation: Interpreted faults show generally north to northeast trends where they offset Santa Fe Group sediments in the central and northern parts of the study area (Fig. 8). Similar to the findings of recent geologic mapping (Koning and Maldonado, 2001; D. Koning, personal commun., 2003), the interpreted faults correspond only in general location and trend to faults mapped by Kelley (1978). Detailed comparisons between the recently mapped faults and the aeromagnetically interpreted faults show good correspondence. A few interpreted faults have no surface expression, which suggests they are buried faults. Some interpreted faults show a single trace that generally corresponds to multiple faults at the surface, implying that the aeromagnetic data reflect the cumulative offsets related to the fault set. Finally, a few mapped faults have no magnetic expression, which suggests that they juxtapose units composed of similar grain size fractions. Analogous relations between mapped and interpreted faults have been observed in the Albuquerque basin (Grauch, 1999).

Faults that can be recognized from the aeromagnetic data are important because the magnetic expression indicates that a major difference in overall lithology occurs on either side of the fault. This difference, which is likely related to grain size, may correspond to a significant contrast in aquifer properties as well. Moreover, the aeromagnetic data can detect faults that juxtapose different units even where there is no surface expression of faulting.

In the southern part of the area, the aeromagnetic data show fewer linear faults within the expression of the Espinaso Formation (F1-F5, Plate 2). The sense of slip on the northwesterly trending fault (F3) can be determined by exposures on its southern end (Lisenbee, 1999). The

two northeasterly faults (F4 and F5) are mostly exposed and likely related to the Tijeras-Cañoncito fault system (Fig. 8; Lisenbee, 1999; Lisenbee and others, 1979). Sense of slip on the entirely buried north-northeast trending faults (F1 and F2) was determined by inspection of magnetic profiles across them. These profiles exhibit forms similar to the thin-thick model of Grauch and others (2001), where the down-thrown thick layer is on the east sides of F1 and F2 and the west side of F3 on its northern end. The throw on this system probably increases to the north, as indicated by increasing depth to the top of the volcanic rocks from the depth contours (Plate 2). Thus, the Ancha Formation likely thickens to the north along the down-thrown side.

Limitations of Results: Interpretations of faults are somewhat ambiguous due to the subjectivity involved in applying the interpretation criteria. The sense of slip cannot be determined for those that offset sediments without detailed modeling and rock-property work. However, this may not be as important for understanding the hydrogeologic framework as knowing whether the faults serve as barriers, conduits, both, or neither.

Recommendations for Future Work: Detailed discussions of the fault interpretations with individual geologists involved in quadrangle mapping would increase our confidence in the fault interpretations. For faults in an area of particular interest, detailed studies and models using ground magnetic data, electrical geophysical data, shallow seismic-reflection data, rock-property measurements, and structural and hydrogeologic analysis, would help characterize the materials on either side of the fault and the fault itself for hydrogeologic importance. The results may indicate how to more directly use geophysical data to predict the hydrogeologic properties near faults.

DIGITAL PRODUCTS

All files are geographically registered using the following map projection parameters: UTM projection, zone 13, NAD27 (Clarke 1866), units in meters.

Image files of Plate 1 and Plate 2 are included as digital files in portable document (PDF) formats for plotting purposes. The pdf files can be viewed on screen or printed from Adobe Acrobat Reader, which is available at no charge from www.adobe.com.

In addition, the color shaded-relief image of the reduced-to-pole magnetic data from Plate 1 is included with minimal annotation in tagged image format (TIF) format for import into GIS programs or use with other overlays. The color shaded-relief images of the aeromagnetic data were derived originally from displays created by ERMAPPER, using a sun azimuth of 270 degrees (west), sun elevation of 60 degrees and nonlinear color scale, which is shown on Plate 1.

The files are briefly described below.

FILENAME	FORMAT TYPE	EXPLANATION
sebmeta.txt		Metadata file describing sebrtp.tif
sebrtp.tif	TIF	Tagged Image Format file of reduced-to-pole aeromagnetic data with tick marks as the only annotation.
sebrtp.tfw	geotif header file	Without the header file, the tif file can be imported into many standard graphics programs. The header file provides geographic information (geotif) for direct import into ARC/INFO and ARC/VIEW. The .tfw file must be in the same directory as the .tif file.
sebrtp.pdf	PDF	Portable document format file for viewing and printing Plate 1 at 1:100,000 scale. Print on a largebed plotter with paper size = ISO A0 (36"X48") in portrait orientation.
seblines.pdf	PDF	Portable document format file for viewing and printing Plate 2 at 1:100,000 scale. Print on a largebed plotter with paper size = ISO A0 (36"X48") in portrait orientation.

ACKNOWLEDGMENTS

Discussions with Gary Smith, Bob Grant, David Sawyer, Adam Read, Alvis Lisenbee, Jack Frost, John Ferguson, Scott Baldridge, John Hawley, and Dan Koning and review by Jeff Phillips have improved the interpretations. This project was the result of joint funding between the USGS National Cooperative Geologic Mapping Program and the New Mexico Office of the State Engineer (NM OSE). Original collection of the aeromagnetic survey over the southern Española basin was in large part funded by the NM OSE.

REFERENCES CITED

Bailey, R. A., Smith, R. L., and Ross, C. S., Stratigraphic omenclature of volcanic rocks in the Jemez Mountains, New Mexico, U. S. Geological Survey Bulletin 1274-P,

Baranov, V., 1957, A new method for interpretation of aeromagnetic maps--pseudogravity anomalies: Geophysics, v. 22, p. 359-383.

Bartolino, J.R., and Cole, J.C., 2002, Ground-water resources of the Middle Rio Grande Basin, New Mexico: U.S. Geological Survey Circular 1222, in press.

Biehler, S., 1999, A geophysical evaluation of the subsurface structure of the Eldorado subdivision, New Mexico: unpublished report for the Eldorado Area Water and Sanitation District, Santa Fe, New Mexico, 40 p.

Biehler, S., Ferguson, J., Baldridge, W. S., Jiracek, G. R., Aldern, J. L., Martinez, M., Fernandez, R., Romo, J., Gilpin, B., Braile, L. W., Hersey, D. R., Luyendyk, B. P., and Aiken, C. L., 1991, A geophysical model of the Española Basin, Rio Grande rift, New Mexico: Geophysics, v. 56, p.340-353.

Blakely, R. J., 1995, Potential theory in gravity and magnetic applications: Cambridge Univ. Press.

Blakely, R. J., and Simpson, R. W., 1986, Locating edges of source bodies from magnetic or gravity anomalies: Geophysics, v. 51, p. 1494-1498.

Borchert, C., and Read, A.S., 1998, Geology of the Tesuque 7.5-min. quadrangle, Santa Fe County, New Mexico, New Mexico Bureau of Mines and Mineral Resources, Open-file Geologic Map OF-GM 47, scale 1:24,000.

Cordell, Lindrith, 1984, Composite residual total intensity aeromagnetic map of New Mexico: National Oceanic and Atmospheric Administration, National Geophysical Data Center. A map of these data for the Albuquerque basin is presented (without complete reference) *in* Pazzaglia, F. J., and Lucas, S. G, Eds., 1999, Albuquerque geology: New Mexico Geological Society Guidebook, 50, p.133.

Cordell, Lindrith, and Grauch, V. J. S., 1985, Mapping basement magnetization zones from aeromagnetic data in the San Juan Basin, New Mexico, *in* Hinze, W. J., Ed., The utility of regional gravity and magnetic maps: Soc. Expl. Geophys., 181-197.

Dethier, D.P., 1997, Geology of White Rock quadrangle, Los Alamos and Santa Fe Counties, New Mexico: New Mexico Bureau of Geology and Mineral Resources Geologic Map GM-73, scale 1:24,000.

Gillespie, C. L., Grauch, V. J. S., Oshetski, Kim, and Keller, G. R., 2000, Principal facts for gravity data collected in the southern Albuquerque basin and a regional compilation, central New Mexico: U. S. Geological Survey Open-File Report 00-490, digital data available from ftp://greenwood.cr.usgs.gov/pub/open-file-reports/ofr-00-240.

Grant, P. R., Jr., 1999, Subsurface geology and related hydrologic conditions, Santa Fe embayment and contiguous areas, New Mexico: New Mexico Geological Society Guidebook, 50, p. 425-435.

Grauch, V.J.S., 1987, A new variable-magnetization terrain correction method for aeromagnetic data: Geophysics, v. 52, no. 1, p. 94-107.

Grauch, V. J. S., 1999, Principal features of high-resolution aeromagnetic data collected near Albuquerque, New Mexico: New Mexico Geological Society Guidebook, 50, 115-118.

Grauch, V. J. S. and Cordell, Lindrith, 1987, Limitations of determining density or magnetic boundaries from the horizontal gradient of gravity or pseudogravity data: Geophysics, v. 52, p. 118-121.

Grauch, V. J. S., Gillespie, C. L., and Keller, G. R., 1999, Discussion of new gravity maps for the Albuquerque basin area: New Mexico Geological Society Guidebook, 50, p. 119124, 2 plates.

Grauch, V. J. S., Hudson, M. R., and Minor, S. A., 2001, Aeromagnetic expression of faults that offset basin fill, Albuquerque basin, New Mexico: Geophysics, v. 66, 707-720.

Grauch, V. J. S., Sawyer, D. A., Fridrich, C. J., and Hudson, M. R., 1997, Geophysical interpretations west of and within the northwestern part of the Nevada Test Site: U. S. Geological Survey Open-File Report 97-496, 45 p.

Haneberg, W. C., 1996, Faults as hydrogeologic units in the Albuquerque basin: New Mexico Bureau of Mines and Mineral Resources Open-File Report 402c, 227 p.

Hansen, R.O., and Simmonds, Marc, 1993, Multiple-source Werner deconvolution: Geophysics, v.58, no.12, p.1792-1800.

Hudson, M. R., Mikolas, Marlo, Geissman, J. W., and Allen, B. D, 1999, Paleomagnetic and rock magnetic properties of Santa Fe Group sediments in the 98th Street core hole and correlative surface exposures, Albuquerque basin, New Mexico: New Mexico Geological Society Guidebook, v. 50, 355-361.

Kautz, P. F., Ingersoll, R. V., Baldridge, W. S., Damon, P. E., and Shafiqullah, M., 1981, Geology of the Espinaso Formation (Oligocene), north-central New Mexico: Summary: Geological Society of America Bulletin, Part I, v. 92, p. 980-983.

Kelley, V. C., 1977, Geology of Albuquerque Basin, New Mexico: New Mexico Bureau of Geology and Mineral Resources Memoir 33.

Kelley, V. C., 1978, Geology of Española basin, New Mexico: New Mexico Bureau of Mines and Mineral Resources Geologic Map 48, scale 1:125,000.

Koning, D.J., 2002, Geology of the Española 7.5-min. quadrangle, Rio Arriba and Santa Fe Counties, New Mexico, New Mexico Bureau of Geology and Mineral Resources, Open-file Geologic Map OF-GM 54, scale 1:24,000.

Koning, D. J. and Hallett, R. B., 2000, Geology of the Turquoise Hill 7.5-min. quadrangle, Santa Fe County, New Mexico, New Mexico Bureau of Mines and Mineral Resources, Open-file Geologic Map OF-GM 41, scale 1:24,000.

Koning, D.J., and Maldonado, F., 2001, Geology of the Horcado Ranch 7.5-min. quadrangle, Santa Fe County, New Mexico, New Mexico Bureau of Geology and Mineral Resources, Open-file Geologic Map OF-GM 44, scale 1:24,000.

Lewis, A.C., and West, F., 1995, Conceptual hydrologic systems for Santa Fe County: New Mexico Geological Society Guidebook, v. 46, p. 299-306.

Lisenbee, A. L., 1999, Geology of the Galisteo 7.5-min. Quadrangle, Santa Fe County, New Mexico, New Mexico Bureau of Mines and Mineral Resources, Open-file Geologic Map OF-GM 30, scale 1:24,000.

Lisenbee, A. L., Woodward, L. A., and Connolly, J. R., 1979, Tijeras-Cañoncito fault system--A major zone of recurrent movement in north-central New Mexico: New Mexico Geological Society Guidebook, 30, p. 89-99.

Manley, K., 1979, Stratigraphy and structure of the Española basin, Rio Grande rift, New Mexico, *in* Riecker, R. E., ed., Rio Grande rift: Tectonics and Magmatism: American Geophysical Union, Washington, D.C., p. 71-86.

Maynard, S., and Lisenbee, A., in press, Geology of the Picture Rock 7.5-min. quadrangle, Santa Fe County, New Mexico, New Mexico Bureau of Mines and Mineral Resources, Open-file Geologic Map OF-GM , scale 1:12,000.

Milsom, J., 1989, Field Geophysics, Geological Society of London Handbook: Halsted Press, New York, 182 pp.

Mozley, P. S., and Goodwin, L. B., 1995, Patterns of cementation along a Cenozoic normal fault: A record of paleoflow orientations: Geology, v. 23, p. 539-542.

Nabighian, M.N., 1972, The analytic signal of two-dimensional magnetic bodies with polygonal cross-section: Its properties and use for automated anomaly interpretation: Geophysics, v. 37, p. 507-517.

Nabighian, M.N., 1974, Additional comments on the analytic signal of two-dimensional magnetic bodies with polygonal cross-section: Geophysics, v. 39, p. 85-92.

Nettleton, L. L., 1971, Elementary gravity and magnetics for geologists and seismologists: Society of Exploration Geophysicists Monograph series, no. 1, 121 p.

Phillips, J.D., 1979, ADEPT--A program to estimate depth to magnetic basement from sampled magnetic profiles: U.S. Geological Survey Open-File Report 79-367, 37 pp.

Phillips, J. D., 1997, Potential-field geophysical software for the PC, version 2.2: U. S. Geological Survey Open-File Report 97-725. Available from http://pubs.usgs.gov/of/1997/ofr-97-0725/

Phillips, J. D, 2000, Locating magnetic contacts: a comparison of the horizontal gradient, analytic signal, and local wavenumber methods: 70th Annual International Meeting, Society of Exploration Geophysicists, Expanded Abstracts, http://seg.org/publications/archive/exAbsHist/abs_pdf/2000/ea200004020405.pdf

Phillips, J. D., 2001, Designing matched bandpass and azimuthal filters for the separation of potential field anomalies by source region and source type: 15th Geophysical Conference and Exhibition, Australian Society of Exploration Geophysicists, Extended Abstracts, CD-ROM.

Phillips, J. D., and Grauch, V. J. S., Editors, in press, Geophysical map interpretation on the PC--A self-paced course using USGS potential-field and image processing software and data for the Getchell gold trend area, Osgood Mountains, Nevada: U. S. Geological Survey Digital Data Series DDS-51.

Read, A.S., Rogers, J., Ralser, S., Ilg, B., Kelley, S., 1999, Geology of the Seton Village 7.5-min quadrangle, Santa Fe County, New Mexico: New Mexico Bureau of Mines and Mineral Resources, Open-file Geologic Map OG-GM 23, scale 1:12,000.

Roest, W.R., and Pilkington, Mark, 1993, Identifying remanent magnetization effects in magnetic data: Geophysics, v. 58, p. 653-659.

Sawyer, D. A., Rodriguez, B. D., Grauch, V. J. S., Minor, S. A., Deszcz-Pan, M., and Thompson, R. A., 1999, Geologic and geophysical data constraining the Cerrillos uplift at the boundary of the Santo Domingo and Española basins, Rio Grande rift, New Mexico: Eos, Transactions, v. 80, no. 46, p. F642.

Sawyer, D. A., Shroba, R. R., Minor, S. A., and Thompson, R. A., 2002, Geologic map of the Tetilla Peak quadrangle, Santa Fe and Sandoval Counties, New Mexico: U. S. Geological Survey Miscellaneous Field Studies Map MF-2352, scale 1:24,000, version 1.0.

Smith, 2000, Oligocene onset of Santa Fe Group sedimentation near Santa Fe, New Mexico [abs.]: New Mexico Geology, v. 22, no.2, p.43.

Smith, G. A., Larsen, D., Harlan, S. S., McIntosh, W. C., Erskine, D. W., and Taylor, S., 1991, A tale of two volcaniclastic aprons: Field guide to the sedimentology and physical volcanology of the Oligocene Espinaso Formation and Miocene Peralta Tuff, north-central New Mexico, *in* Julian, B. and Zidek, J., Field guide to geologic excursions in New Mexico and adjacent areas of Texas and Colorado: New Mexico Bureau of Mines and Mineral Resources Bulletin 137, p. 87-103.

Smith, R.S., Thurston, J.B., Dai, Ting-Fan, and MacLeod, I.N., 1998, iSPI™ - the improved source parameter imaging method: Geophysical Prospecting, v. 46, p. 141-151.

Spiegel, Z., and Baldwin, B., 1963, Geology and water resources of the Santa Fe area, New Mexico: U. S. Geological Survey Water-supply Paper 1525, 258 pp.

Sun, M. and Baldwin, B., 1958, Volcanic rocks of the Cienega area, Santa Fe County, New Mexico: New Mexico Bureau of Mines and Mineral Resources Bulletin 54, 80 pp.

Sweeney, R. E., Grauch, V. J. S., and Phillips, J. D., 2002, Merged digital aeromagnetic data for the Albuquerque and southern Española Basins, New Mexico: U. S. Geological Survey Open-File Report 02-205, available on-line at http://pubs.usgs.gov/of/2002/ofr-02-0205.

Syberg, F. J. R., 1972, A Fourier method for the regional-residual problem of potential fields: Geophys. Prosp., v. 20, p. 47-75.

Thompson, D.T., 1982, EULDPH: A new technique for making computer-assisted depth estimates from magnetic data: Geophysics, v. 47, p. 31-37.

Thompson, R. A., Minor, S. A., and Sawyer, D. A., 1997, The Cerros del Rio volcanic field and the La Bajada fault system—geologic overview and status report: U. S. Geological Survey Open-File Report 97-116, p. 26-27.

Thurston, J.B., and Smith, R.S., 1997, Automatic conversion of magnetic data to depth, dip, and susceptibility contrast using the SPI™ method: Geophysics, v. 62, p. 807-813.

U. S. Geological Survey, Sander Geophysics, Ltd., and Geoterrex, 1999, Digital data from the Sandoval-Santa Fe, Belen, and Cochiti aeromagnetic surveys, covering areas in Sandoval, Santa Fe, Rio Arriba, Valencia, and Socorro Counties, New Mexico: U. S. Geological Survey Open-File Report 99-404.

Table 1. Explanation of elements of the profile models and their corresponding physical properties (Fig. 4).

Unit code	Description	Density g/cm^3	Magnetic Suscept. (SI)	Comments
QTb	Cerros del Rio basalts	2.57	-0.015	1. Reverse-polarity remanence is represented by negative susceptibility 2. Independent analysis shows basalts are not extensive at depth on the west side (Plate 2).
SFG/ SFGdeep	Quaternary-Tertiary Santa Fe Group, primarily Ancha and Tesuque Formations shallow/deep	2.17/ 2.30	0.0	1. Density-depth function that increases from 2.17 to 2.30 g/cm^3 at about 4100 ft (1.25 km) depth was chosen based on examination of borehole density logs for the region. 2. Magnetic susceptibility set to zero because it is negligible in this model compared to other units.
Tov	Oligocene volcanic and related rocks (generally the Espinaso Formation and Cieneguilla basanite), which includes volcaniclastic and tuffaceous rocks, breccias, and flows. Vents are not well resolved in the model.	2.42	0.01	1. Density based on limited information from borehole density logs. 2. Magnetic susceptibility is compatible with measured values on a few hand samples of Espinaso Fm.
sed rocks	Undifferentiated, pre-Santa Fe Group sedimentary rocks, excluding the limestone-dominated Paleozoic Madera Group, which rests directly on Precambrian basement. The section is variably eroded and may be entirely absent in parts of the model area.	2.47	0.0	Density is compatible with borehole density logs from Albuquerque basin for Eocene Galisteo Formation and Mesozoic sedimentary rocks.
PC/Madera	Average Precambrian basement rocks with low to medium magnetization, which cannot be distinguished from estimated physical properties of limestone-dominated Madera Group.	2.67	0.0	1. Rocks of average crustal density. 2. Rocks with magnetic susceptibilities less than 0.01 are all represented by zero susceptibility. Using nonzero susceptibilities would not change the overall character of the modeled results because the unit occurs generally > 5000 ft (~1.5 km) deep in the model.
PC-mag	Highly magnetic Precambrian basement rocks.	2.67	0.05	Rocks of average crustal density and very high magnetic susceptibilities that likely are proxies for additional remanence and/or added volume at depth.
PC-mod	Moderately magnetic Precambrian basement rocks.	2.67	0.02 - 0.03	Rocks of average crustal density and magnetic susceptibilities similar to the highest values measured on several samples of Precambrian gneiss (M. Hudson, unpub. data, 2002). The variation in magnetic susceptibility is used in the model to represent a gradual decrease in magnetic susceptibility to the east.

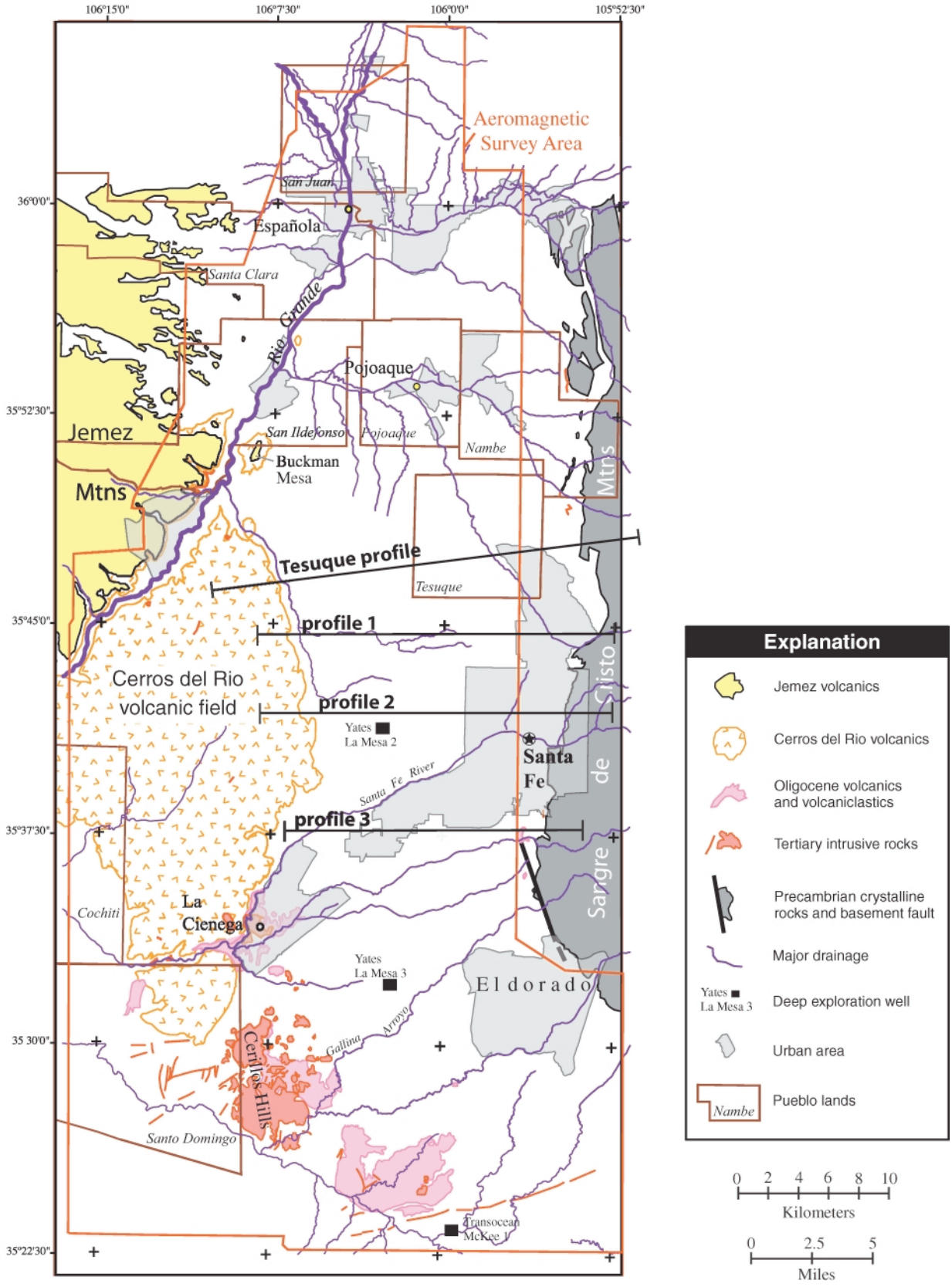

Figure 1. Location of the aeromagnetic survey area in the southern Española basin area. Selected geographic features are also shown, such as cities and urban areas, Pueblo boundaries, and major drainages. See Plate 1 for additional geographic features. Geologic contacts are from Kelley (1978).

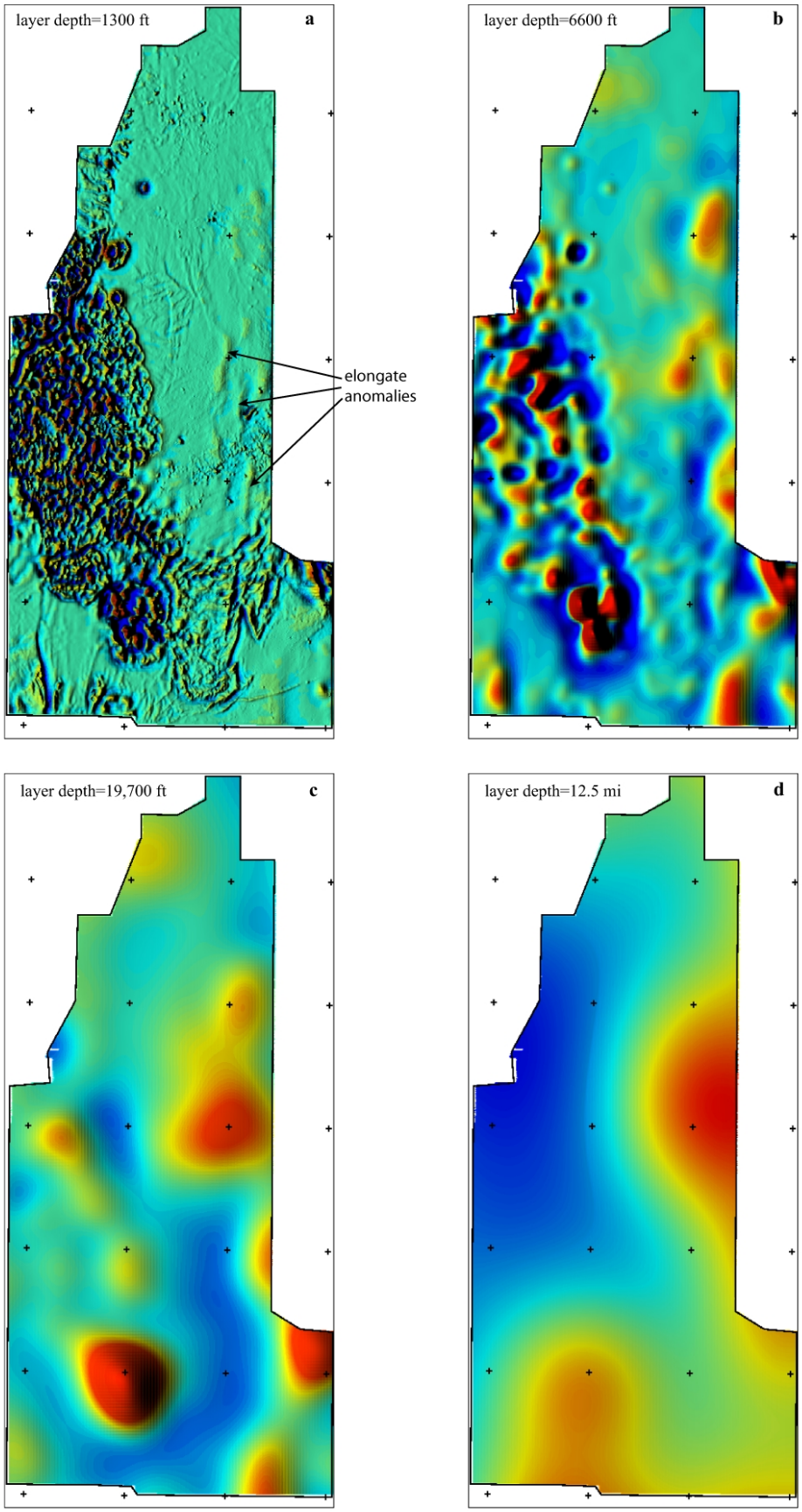

Figure 2. Results of matched filtering (Phillips, 2001) to separate the reduced-to-pole aeromagnetic data (Plate 1) into different depth components. Anomalies were separated based on their match to a dipole layer at 0.4 km (1300 ft) (a), at 2.0 km (6600 ft) (b), at 6 km (19,700 ft) (c), and to a half-space at 20 km (12.5 miles) (d). Note the presence of different aspects of basement-related anomalies (Fig. 5) and the Cerrillos intrusion (Fig. 6) in all four components. The shallowest depth component (a) was used for interpretation of faults.

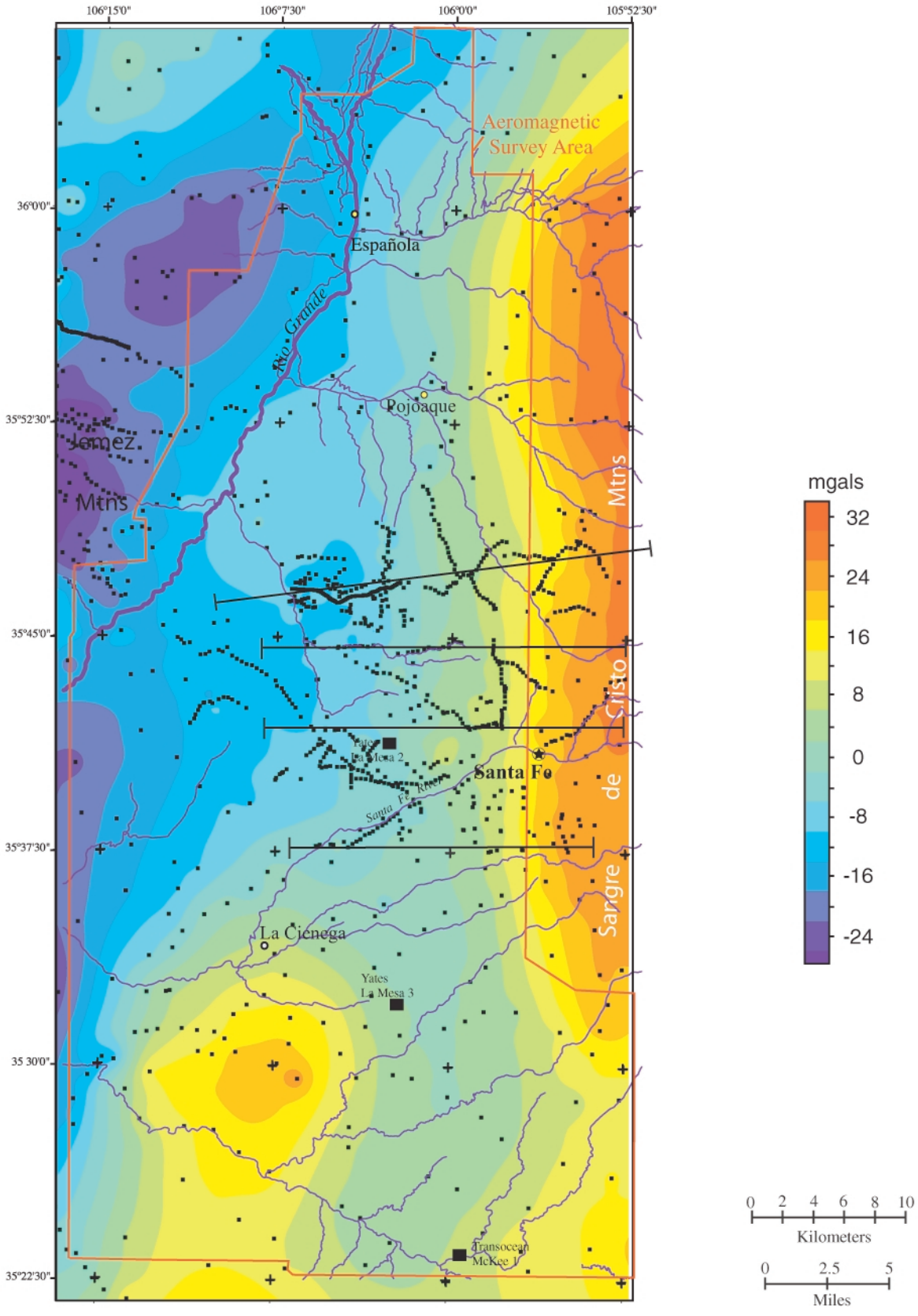

Figure 3. Isostatic residual gravity map for the study area, showing locations of gravity stations (small black squares). Data are from Gillespie and others (2000).

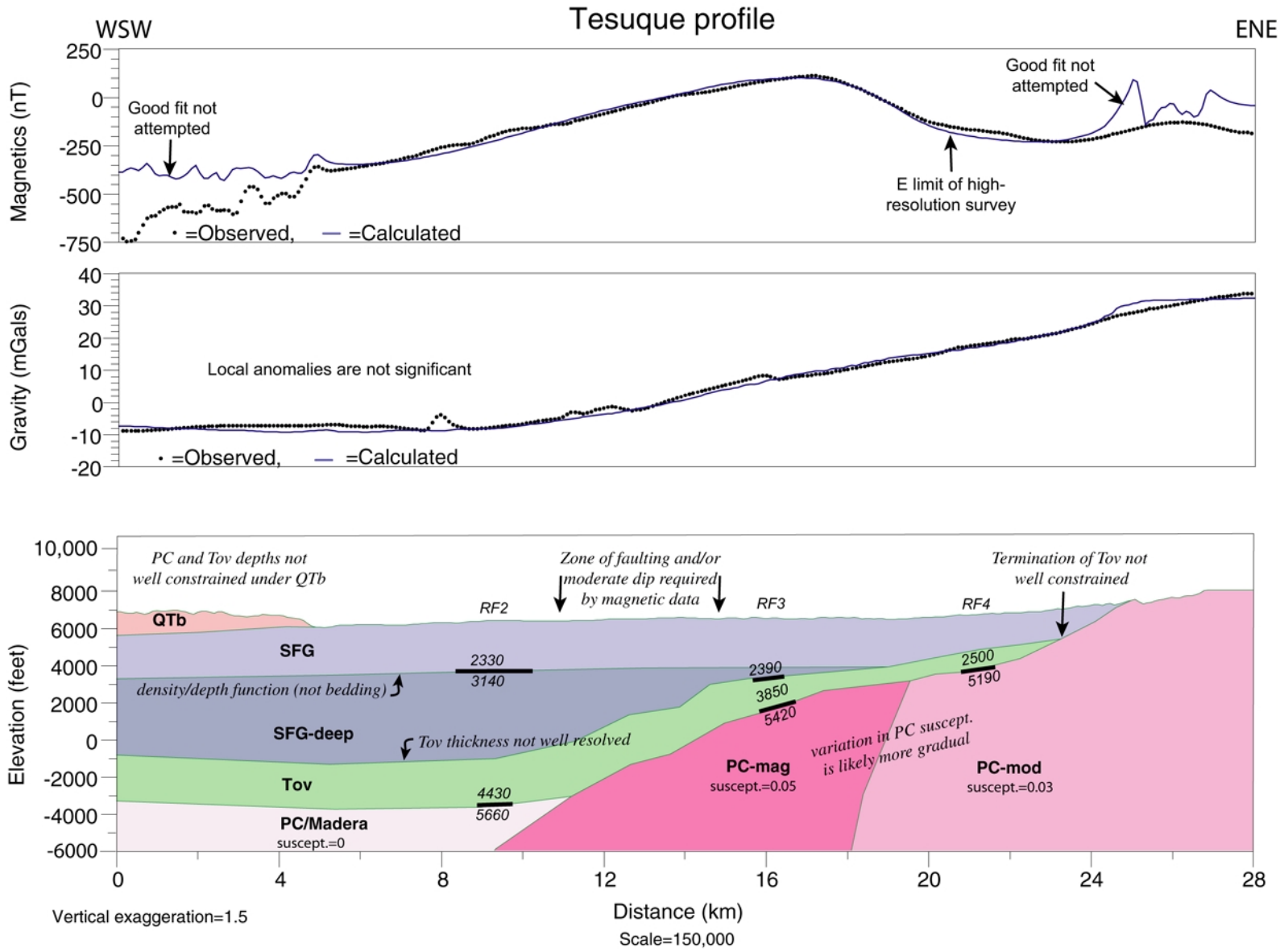

Figure 4a. Geophysical model for the Tesuque profile (located on Fig.1). Model units and their physical properties are described in Table 1. Susceptibilities (suscept.) in SI units are shown for Precambrian basement rocks only. Bold lines are seismic refraction interfaces (labeled RF2, RF3, RF4) from Biehler and others (1991), showing velocities in m/sec^2 for the layers above and below the interfaces. General constraints were provided by geologic considerations (Borchert and Read, 1998; Koning and Maldonado, 2001; Koning, personal commun., 2003) and preliminary information from seismic reflection data (J. Ferguson, personal commun., 2002).

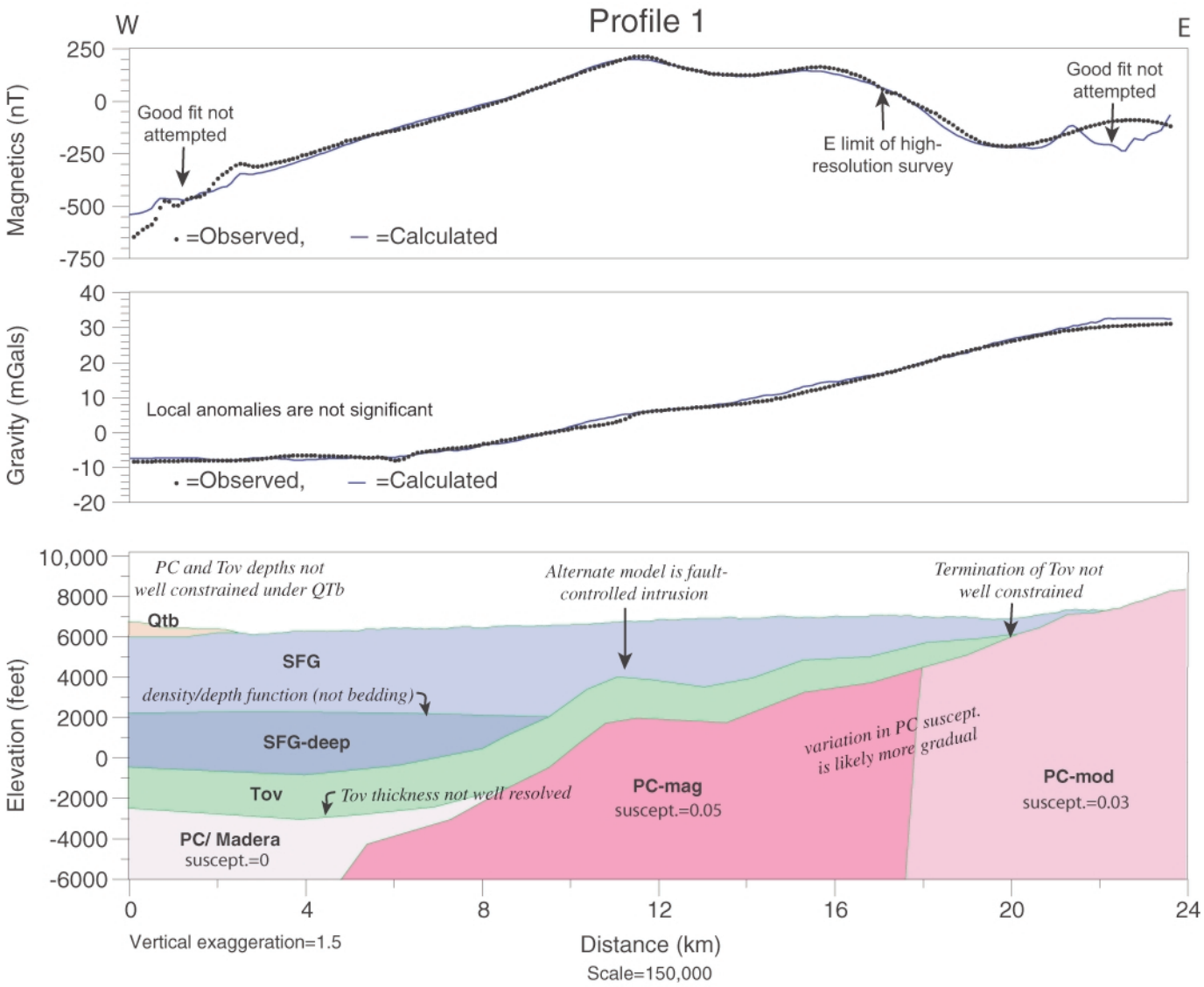

Figure 4b. Geophysical model for profile 1 (located on Fig.1). Model units and their physical properties are described in Table 1. Magnetic susceptibilities (suscept.) in SI units are shown for Precambrian basement rocks only. Additional constraints were provided by magnetic depth estimation (not shown) and preliminary subsurface interpretations (D. Koning, personal commun., 2003).

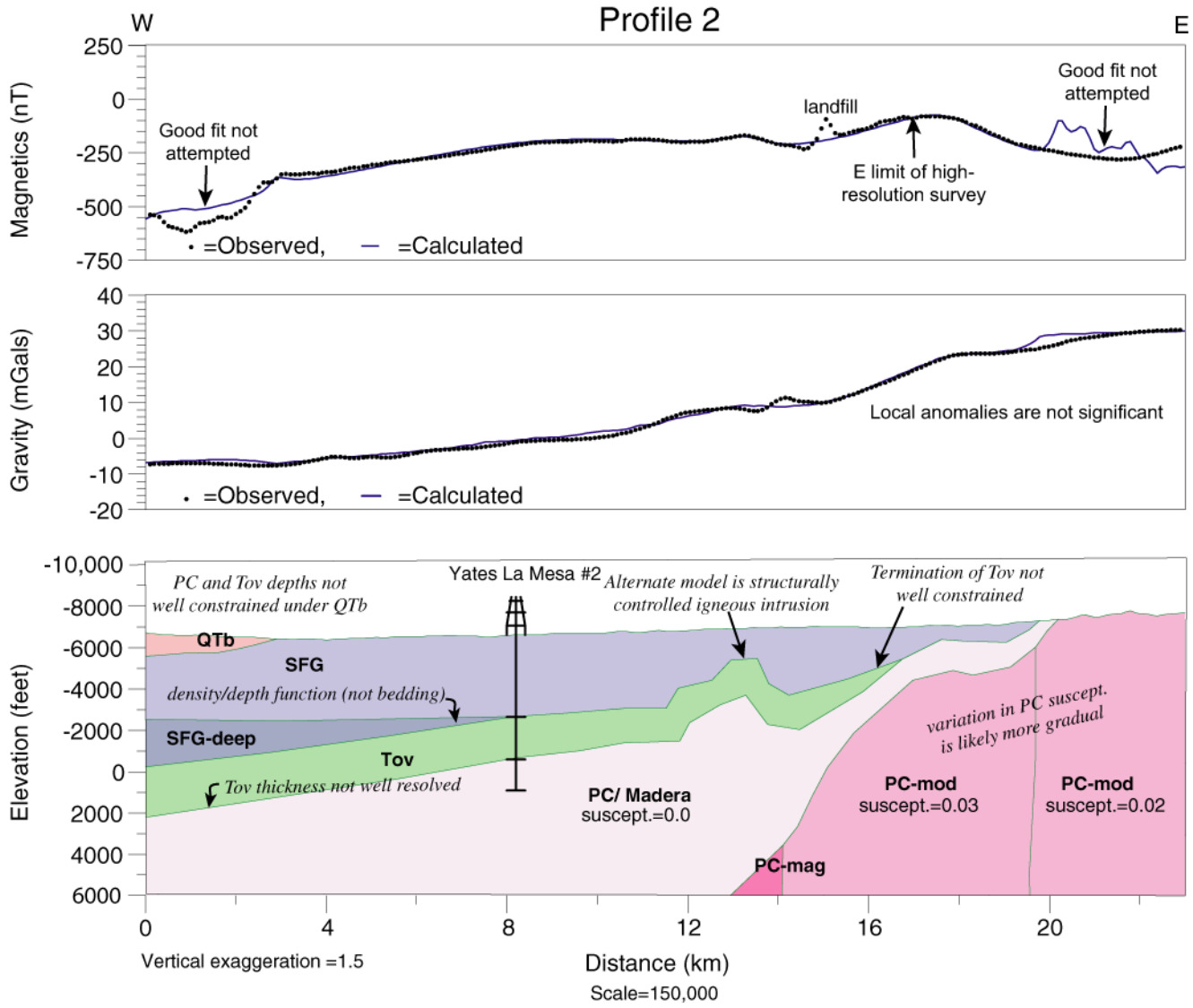

Figure 4c. Geophysical model for profile 2 (located on Fig.1). Model units and their physical properties are described in Table 1. Densities (d) in cgs units of g/cm3 and magnetic susceptibilities (s) in SI units are shown for Precambrian basement rocks only. Constraints are provided by the Yates La Mesa #2 (YLM #2) exploration well. Additional constraints on depths were provided from SAGE proprietary seismic-reflection data (not shown).

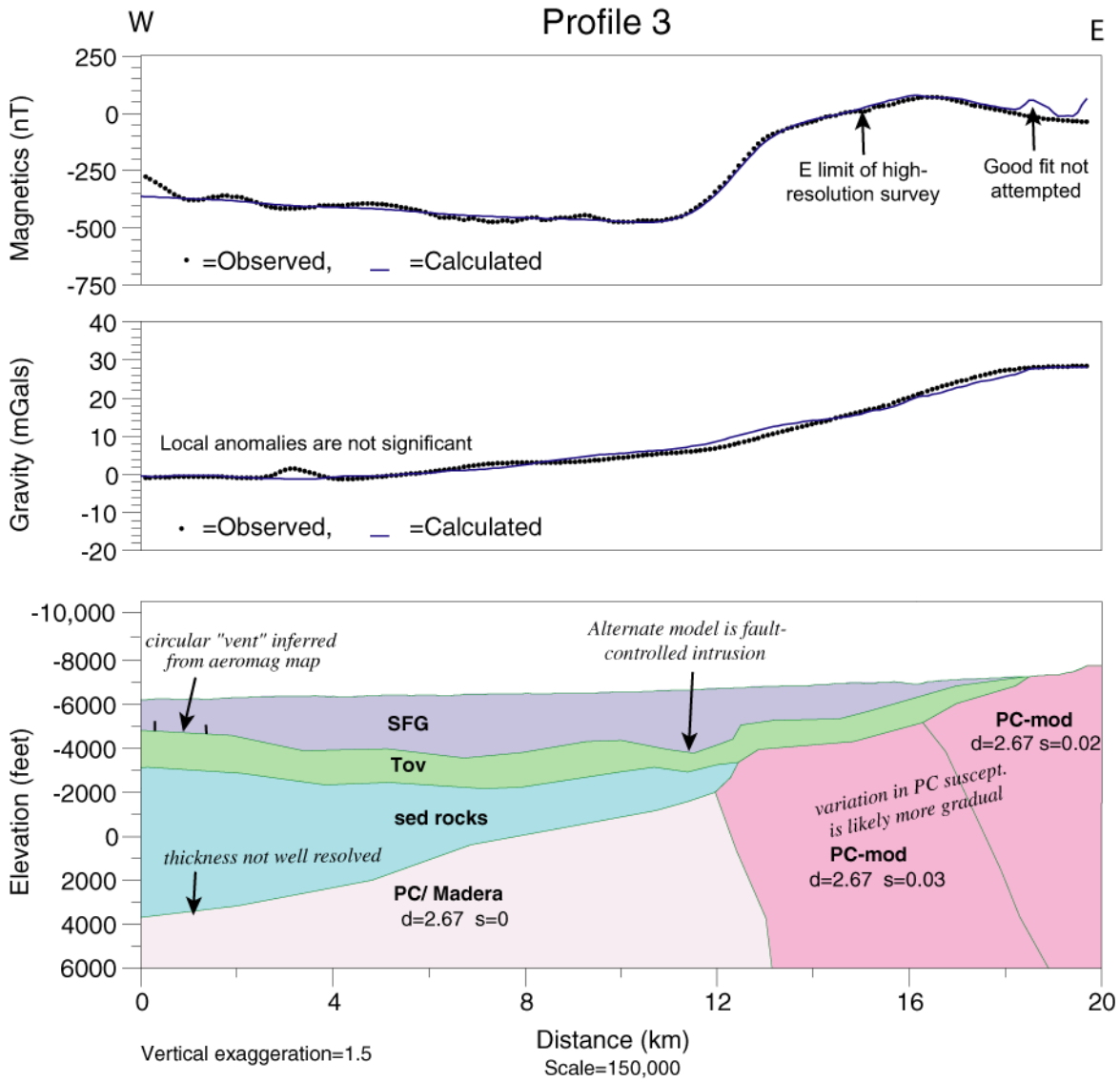

Figure 4d. Geophysical model for profile 3 (located on Fig.1). Model units and their physical properties are described in Table 1. Densities (d) in cgs units of g/cm3 and magnetic susceptibilities (s) in SI units are shown for Precambrian basement rocks only. The vent marked at the top of Tov unit was located from depth-estimate analysis and map interpretation of the aeromagnetic data (Plate 2). Additional constraints on depths were provided from SAGE proprietary seismic-reflection data (not shown).

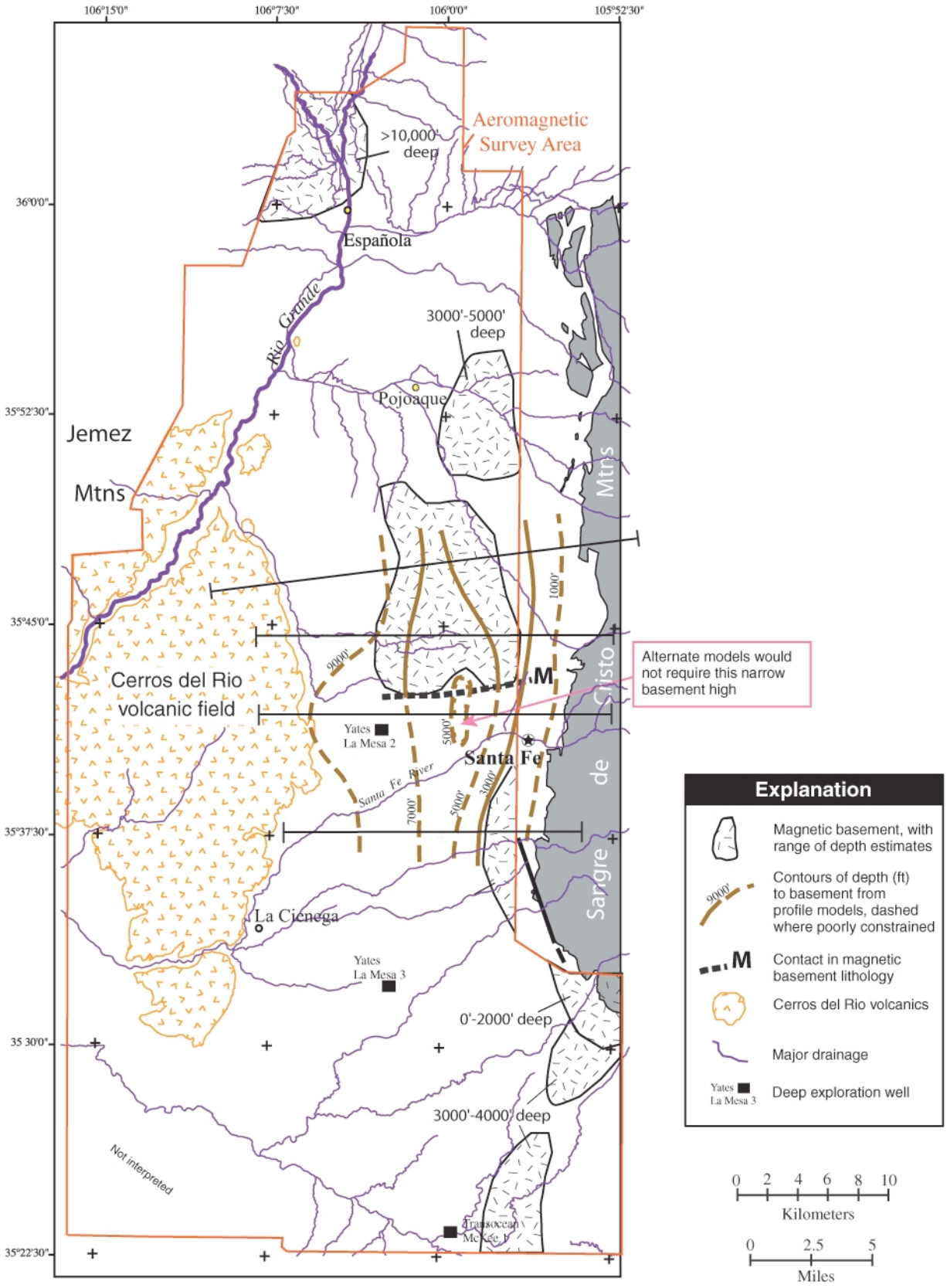

Figure 5. Interpretation of Precambrian basement. The general outlines of aeromagnetic anomalies likely associated with magnetic Precambrian basement and expected depth ranges are shown. Depth contours were derived from the geophysical profile models (Fig. 4). Alternate models (discussed in text) would depict a Tertiary intrusion in place of the narrow basement highs, giving a more consistent slope to the basement surface. Depth contours near the Eldorado area are shown on Plate 2. The southern termination of the anomaly north of Santa Fe (M) is likely due to a contrast in magnetic lithology (see text).

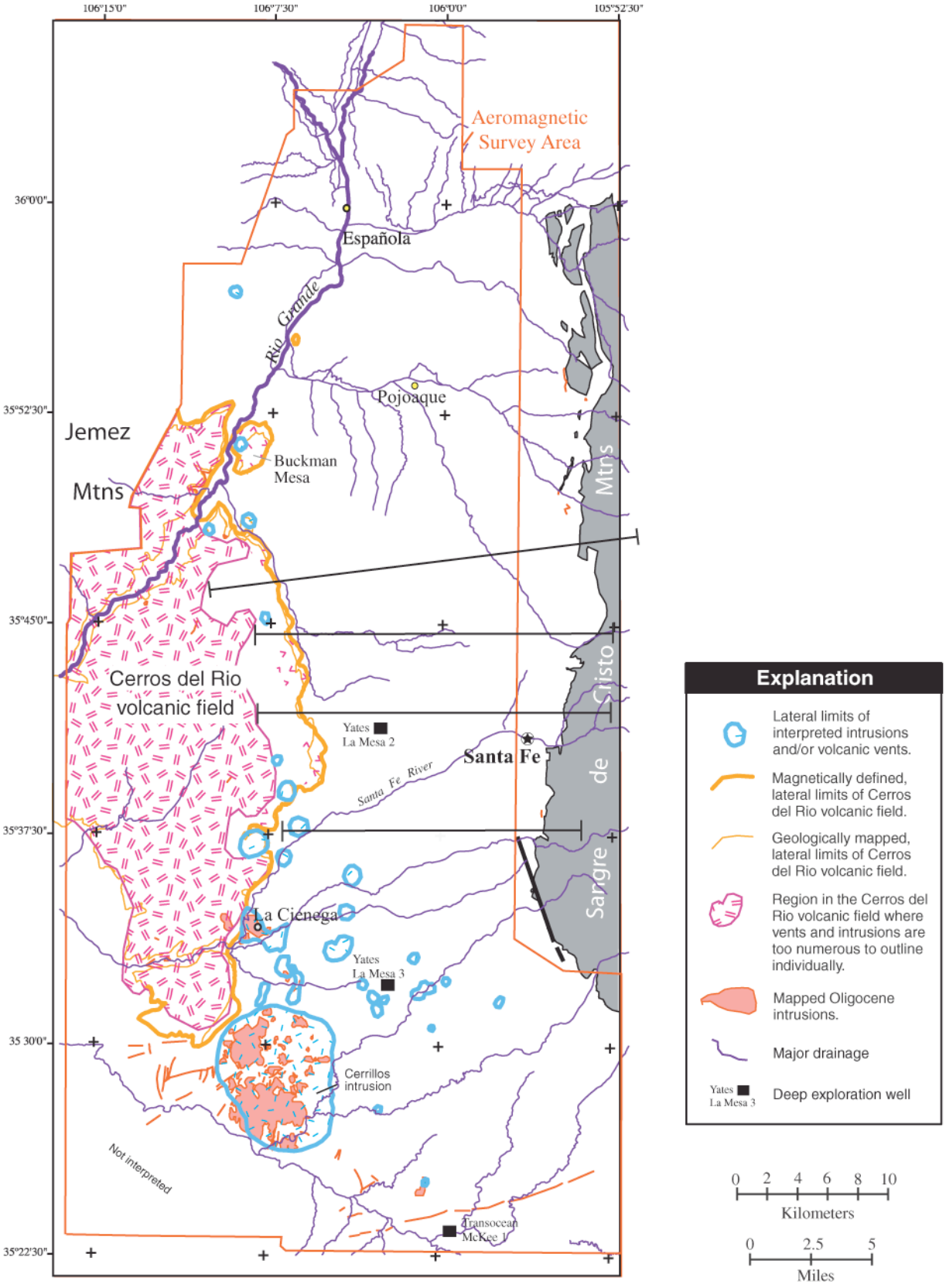

Figure 6. Interpretation of intrusions, volcanic vents, and the limit of Cerros del Rio volcanic field in relation to exposed Tertiary intrusive rocks (see explanation). Depth estimates to the intrusions are given on Plate 2. The lateral limits of individual intrusions and volcanic vents are outlined, except in the area where they are too numerous to distinguish (vent area). In this volcanic vent area, basaltic rocks are probably voluminous and reach great depths. Volcanic vents(?) in the southern part of the area are inferred to be Oligocene in age, because their depths are similar to the depths estimated for Oligocene rocks nearby (Plate 2). Geologic contacts from Kelley (1978).

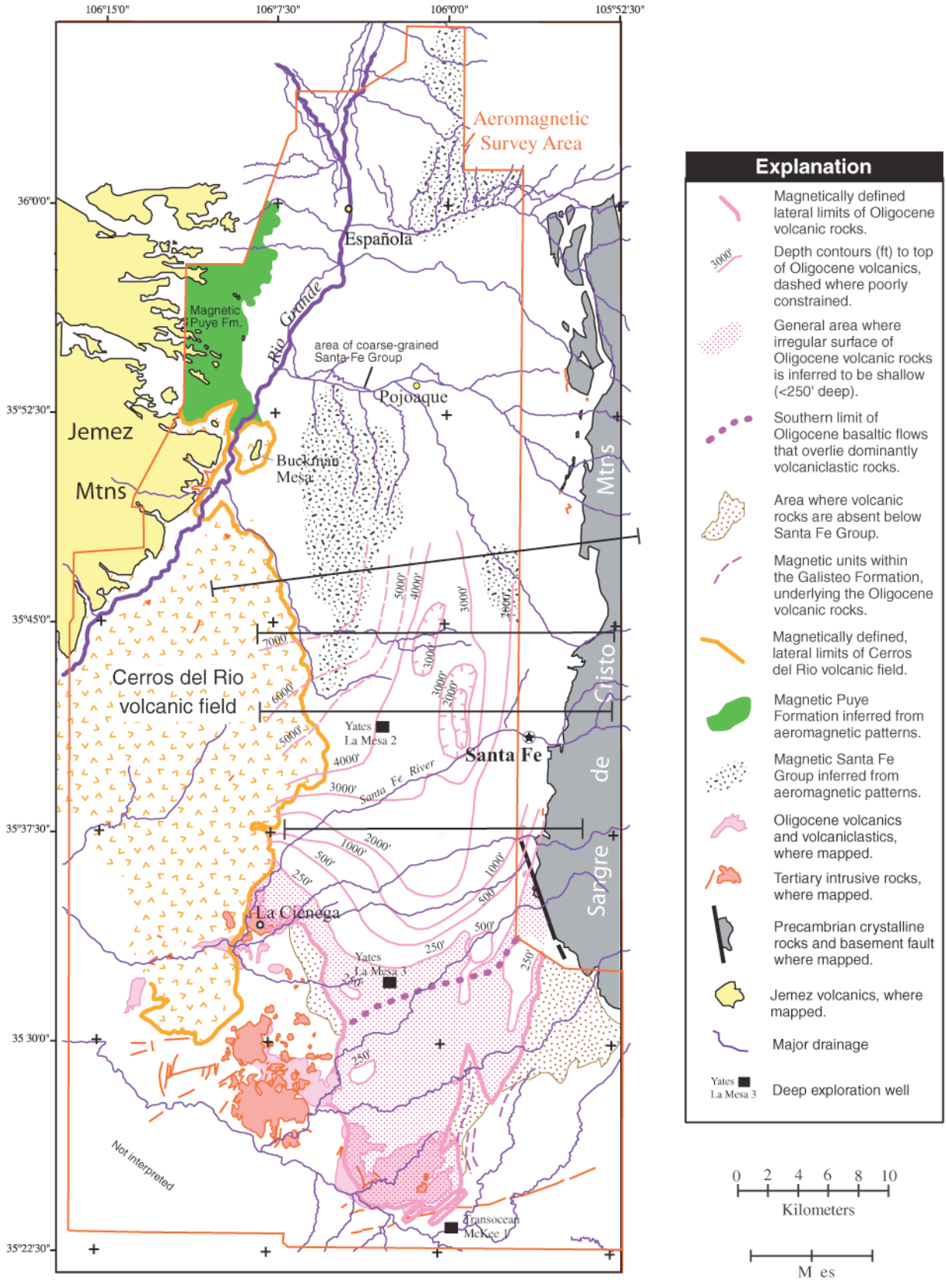

Figure 7. Interpretation of Oligocene volcanic rocks in relation to exposed Oligocene intrusive and volcanic rocks. See explanation. Depths of the contours are labeled on Plate 2. See explanation for other features. Geologic contacts from Kelley (1978).

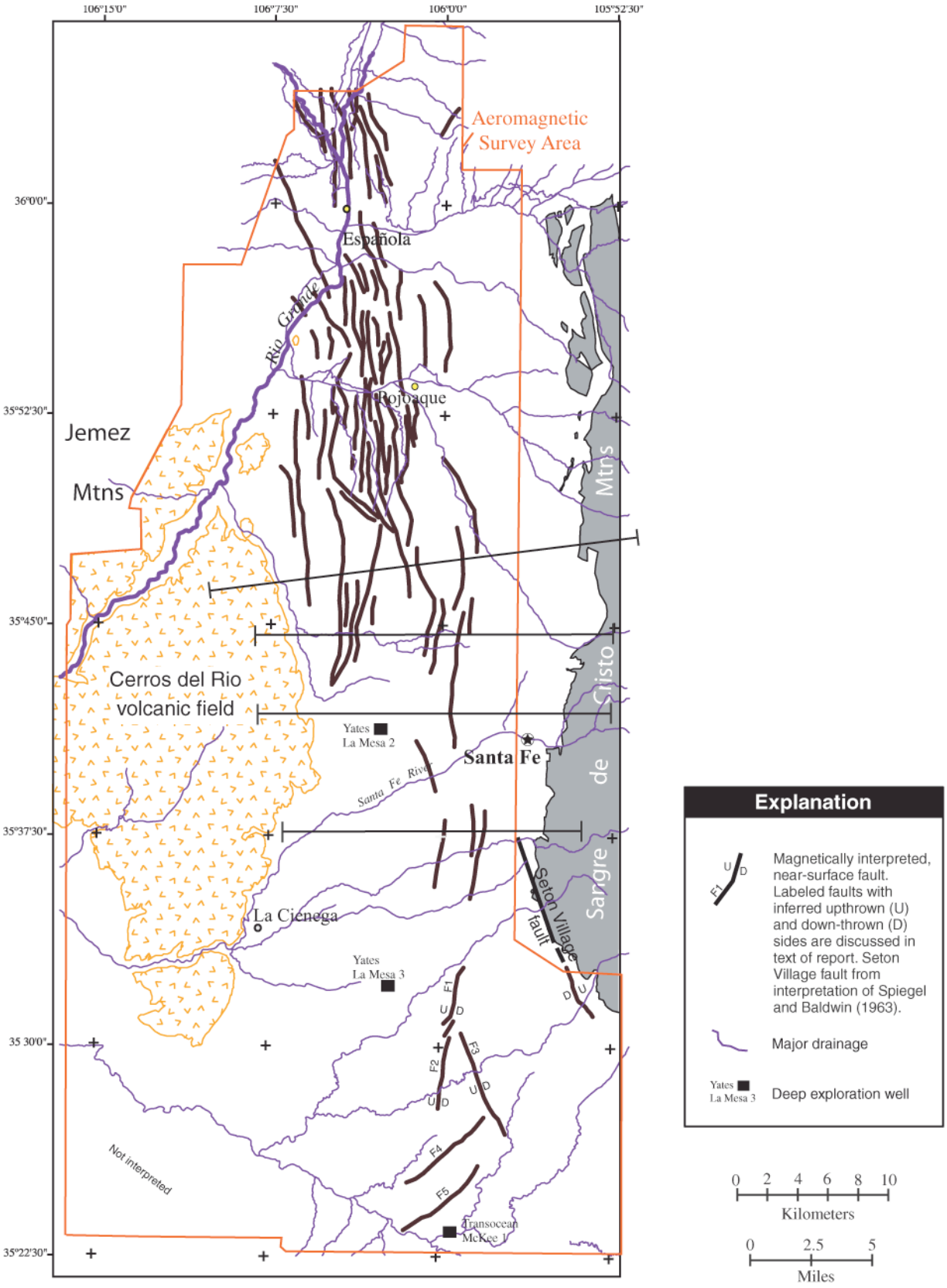

Figure 8. Interpretation of shallow faults (thick black lines), following the criteria discussed in text. The shallow basement fault in the northeastern Eldorado area aligns with the Seton Village fault of Spiegel and Baldwin (1963).